Canad. J. Math. Vol. 78 (5), 2026 pp. 1738–1765
http://dx.doi.org/10.4153/S0008414X25000094
© The Author(s), 2025. Published by Cambridge University Press on behalf of Canadian Mathematical Society. This is an Open Access article, distributed under the terms of the Creative Commons Attribution-NonCommercial licence (https://creativecommons.org/licenses/by-nc/4.0/), which permits non-commercial re-use, distribution, and reproduction in any medium, provided the original work is properly cited. The written permission of Cambridge University Press must be obtained for commercial re-use.

# Pebble trees

Vincent Pilaud

*Abstract.* A pebble tree is an ordered tree where each node receives some colored pebbles, in such a way that each unary node receives at least one pebble, and each subtree has either one more or as many leaves as pebbles of each color. We show that the contraction poset on pebble trees is isomorphic to the face poset of a convex polytope called pebble tree polytope. Beside providing intriguing generalizations of the classical permutahedra and associahedra, our motivation is that the faces of the pebble tree polytopes provide realizations as convex polytopes of all assocoipahedra constructed by K. Poirier and T. Tradler only as polytopal complexes.

## 1 Introduction

Permutahedra and associahedra are among the most classical polytopes in algebraic combinatorics. The $(n-1)$-dimensional permutahedron has a vertex for each permutation of $[n] := \{1, \dots, n\}$ and an edge for each pair of permutations related by the transposition of two adjacent entries. The $(n-1)$-dimensional associahedron has a vertex for each binary tree on $n$ nodes and an edge for each pair of binary trees related by a rotation. These two families of polytopes admit common generalizations explaining their similar behavior, including the permutreehedra of [PP18], the quotientopes of [PS19], and the $(m, n)$-multiplihedra of [CP22]. All these polytopes are actually deformed permutahedra (defined as generalized permutahedra in [Pos09, PRW08]), meaning that their normal fans all coarsen the braid fan. This article is devoted to another common generalization to the permutahedra and associahedra, which are not deformed permutahedra in general.

The combinatorics of this generalization is based on pebble trees. A *pebble tree* is an ordered tree where each node receives some colored pebbles in such a way that each unary node receives at least one pebble, and each subtree has either one more or as many leaves as pebbles of each color (see Figure 1 and the more precise Definition 2.1). We consider the set of pebble trees with a fixed number of leaves and fixed sets of unbalanced and balanced colors (*i.e.,* the colors for which the number of leaves equals

Received by the editors May 16, 2024; revised November 26, 2024; accepted February 3, 2025.
Published online on Cambridge Core February 10, 2025.
Partially supported by the Spanish project PID2022-137283NB-C21 of MCIN/AEI/10.13039/501100011033 / FEDER, UE, by the Spanish–German project COMPOTE (AEI PCI2024-155081-2 & DFG 541393733), by the Severo Ochoa and María de Maeztu Program for Centers and Units of Excellence in R&D (CEX2020-001084-M), by the Departament de Recerca i Universitats de la Generalitat de Catalunya (2021 SGR 00697), by the French project CHARMS (ANR-19-CE40-0017), and by the French–Austrian project PAGCAP (ANR-21-CE48-0020 & FWF I 5788).
AMS subject classification: **05C05**, **05E99**, **52B11**, **52B12**, **05A15**.
Keywords: Trees, polytopes, permutahedra, associahedra.

https://doi.org/10.4153/S0008414X25000094 Published online by Cambridge University Press

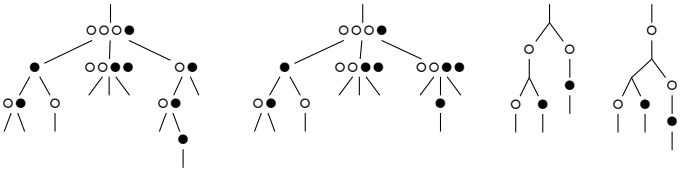


*Figure 1*: Some ∘-balanced and •-unbalanced $\{\circ, \bullet\}$-pebble trees. The first two are related by a contraction (Section 2.2), while the last two are related by a flip (Section 2.4).

or exceeds the number of pebbles). It is immediate from the definition that these pebble trees are closed by arc contractions, and our main result is that the contraction poset is the face poset of a simple convex polytope, that we call the *pebble tree polytope* (see Figure 14). For this, we first construct the *pebble tree fan*, associating to each pebble tree a polyhedral cone in a natural but subtle way, and then prove that this fan is the normal fan of a polytope by checking that its wall-crossing inequalities are satisfiable.

Our construction recovers the combinatorics and geometry of the permutahedra and associahedra in two degenerate situations. On the one hand, pebble trees with a single leaf can be seen as ordered partitions of their balanced colors, and the pebble tree polytope is the permutahedron. On the other hand, pebble trees with no pebbles are Schröder trees, and the pebble tree polytope is the associahedron. But the special situation which motivated this article is when there is exactly one color of pebbles. The pebble trees are then in bijection with some specific oriented planar trees considered by K. Poirier and T. Tradler in [PT18] for the combinatorics of algebraic structures endowed with a binary product and a co-inner product. These structures are closely connected to the $V_\infty$-algebras of T. Tradler and M. Zeinalian [TZ07] that arose in a tentative algebraic model for string topology operations defined by M. Chas and D. Sullivan [CS99]. It is proved in [PT18] that the contraction posets on these oriented planar trees are face lattices of the *assocoipahedra*, which are polytopal complexes refining the boundary complex of the Cartesian product of an associahedron with a simplex. We prove here that all assocoipahedra can actually be realized as convex polytopes using faces of pebble tree polytopes (see Figure 15).

The paper is organized as follows. Section 2 is devoted to the combinatorics of pebble trees. In Section 2.1, we provide more precise definitions and notations for pebble trees, we introduce some natural maps between families of pebble trees, and we give the precise bijection with the oriented planar trees of [PT18]. We introduce in Section 2.2 the pebble tree contraction poset, prove in Section 2.3 that it is the face poset of a pseudomanifold called the pebble tree complex, and discuss in Section 2.4 the adjacency graph of this complex called the pebble tree flip graph. Section 3 is devoted to the geometry of pebble trees. After quickly reminding the reader some geometric preliminaries in Section 3.1, we construct the pebble tree fan in Section 3.2 and the pebble tree polytope in Section 3.3. Finally, Section 4 is devoted to the numerology of pebble trees. We compute the generating functions of the maximal pebble trees in Section 4.1 and of all the pebble trees in Section 4.2, and gather explicit expansions of these generating functions in Section 4.3. While the methods are

https://doi.org/10.4153/S0008414X25000094 Published online by Cambridge University Press

standard computations based on generatingfunctionology [FS09], the results reveal a few surprises.

## 2 Pebble tree combinatorics

In this section, we define pebble trees (Section 2.1) and study the pebble tree contraction poset (Section 2.2), the pebble tree complex (Section 2.3), and the pebble tree flip graph (Section 2.4).

### 2.1 Pebble trees

Recall that an *ordered tree* is either a *leaf* or a *node* with an ordered list of subtrees. These subtrees are the *children* of the node, and this node is the *parent* of these subtrees. As we only consider ordered trees, we omit the adjective ordered and only say tree. For a node $n$ in a tree $T$, we denote by $T_n$ the subtree of $T$ rooted at $n$. For a subtree $S$, we denote by $\mathsf{L}(S)$ the set of leaves of $S$.

***Definition 2.1*** For a finite set of colors $\Gamma$, a *$\Gamma$-pebble tree* is a tree with pebbles colored by $\Gamma$ placed on its nodes such that

(1) each leaf receives no pebble, each node with a single child receives at least one pebble, and each node with at least two children receives arbitrary many pebbles (possibly none),
(2) for each subtree $S$ and each color $\gamma \in \Gamma$, the number of leaves minus the number of pebbles of color $\gamma$ in $S$ is either 0 or 1.

***Example 2.1*** Two classical combinatorial objects are extreme examples of pebble trees:

- pebble trees with a single leaf can be seen as ordered partitions of their pebble colors,
- pebble trees with no pebbles (meaning $\Gamma = \varnothing$) are Schröder trees (where each node has either none or at least two children).

Some more generic examples of pebble trees are illustrated in Figure 1. Note that all our pictures of trees start with a vertical half-edge attached to the root, and end with half-edges representing the leaves.

***Notation 2.2*** *We call $\gamma$-pebbles the pebbles of color $\gamma$. We call $\gamma$-pebble default of a subtree $S$ the difference $\Delta_\gamma(S)$ between the number of leaves and the number of $\gamma$-pebbles of $S$. We say that $S$ is $\gamma$-balanced (resp. $\gamma$-unbalanced) if $\Delta_\gamma(S) = 0$ (resp. $\Delta_\gamma(S) = 1$). We denote by $\mathsf{B}(S) := \{\gamma \in \Gamma \mid \Delta_\gamma(S) = 0\}$ (resp. $\mathsf{U}(S) := \{\gamma \in \Gamma \mid \Delta_\gamma(S) = 1\}$) the set of colors $\gamma \in \Gamma$ for which $S$ is $\gamma$-balanced (resp. $\gamma$-unbalanced).*

***Notation 2.3*** *We denote by $\mathcal{P}_L^\Gamma$ the set of all pebble trees with leaves $L$ and pebble colors $\Gamma$, and by $\mathcal{P}_L^{B,U}$ the subset of $B$-balanced and $U$-unbalanced pebble trees of $\mathcal{P}_L^\Gamma$ for any $B \sqcup U = \Gamma$. For $\ell, b, u \in \mathbb{N}$, we define $\mathcal{P}_\ell^{b,u}$ as $\mathcal{P}_{[\ell]}^{[b],[b+1,b+u]}$. In this case, we label the leaves by $[\ell]$ from left to right, the balanced pebble colors by $[b]$ and the unbalanced pebble colors by $[b+1, b+u]$. Note that $\mathcal{P}_L^{B,U}$ is isomorphic to $\mathcal{P}_\ell^{b,u}$ for arbitrary $L, B, U$ with $|L| = \ell$, $|B| = b$ and $|U| = u$. It is however convenient to keep the notation $\mathcal{P}_L^{B,U}$ to define certain operations on pebble trees (see Definitions 2.2–2.5) and for recursive decompositions of the pebble trees (see Section 4).*

https://doi.org/10.4153/S0008414X25000094 Published online by Cambridge University Press

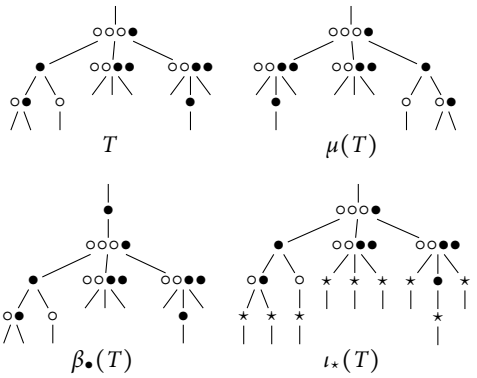



*Figure 2*: A ∘-balanced and •-unbalanced $\{\circ,\bullet\}$-pebble tree (left), the ∘-balanced and •-unbalanced $\{\circ,\bullet\}$-pebble tree obtained by mirroring it (middle left), the $\{\circ,\bullet\}$-balanced $\{\circ,\bullet\}$-pebble tree obtained by •-balancing it (middle right), and the $\{\circ,\star\}$-balanced and •-unbalanced $\{\circ,\bullet,\star\}$-pebble tree obtained by $\star$-inserting it (right).

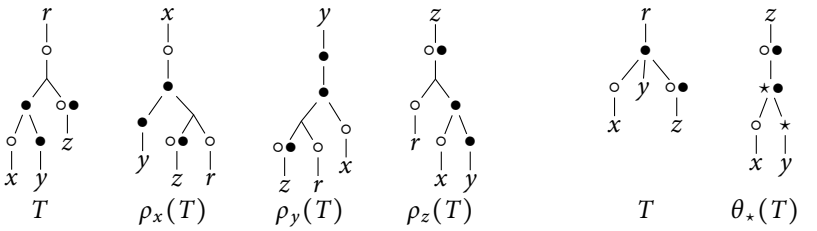



*Figure 3*: A fully balanced $\{\circ,\bullet\}$-pebble tree and the fully balanced $\{\circ,\bullet\}$-pebble trees obtained by rerooting it at leaves $x$, $y$ and $z$ respectively (left). A fully unbalanced $\{\circ,\bullet\}$-pebble tree and the fully balanced $\{\circ,\bullet,\star\}$-pebble tree obtained by $\star$-uprooting it (right).

***Remark 2.4*** Some immediate consequences of Definition 2.1:

- $\mathcal{P}_L^\Gamma$ is finite for any $L$ and $\Gamma$, thus $\mathcal{P}_\ell^{b,u}$ is finite for any $\ell, b, u \in \mathbb{N}$.
- The number of $\gamma$-pebbles at a node $p$ with children $c_1, \dots, c_k$ is $\left(\sum_{i=1}^k \Delta_\gamma(T_{c_i})\right) - \Delta_\gamma(T_p)$. Hence, the number of $\gamma$-unbalanced children of $p$ is the number of $\gamma$-pebbles at $p$, plus 1 if $p$ is $\gamma$-unbalanced.
- Each unary node has at least one pebble, and at most one of each color.
- There is no consecutive chain formed by $|\Gamma| + 1$ unary nodes

We now define five natural maps between pebble trees (see Figures 2 and 3), that will induce isomorphisms in Propositions 2.10, 2.17, and 3.11. In Definitions 2.4 and 2.6, we call $\gamma$-leaf the only pebble tree of $\mathcal{P}_1^{\{\gamma\},\varnothing}$, *i.e.,* whose root has a single pebble of color $\gamma$ and a single child which is a leaf.

***Definition 2.2*** The *mirroring map* sends a pebble tree $T$ of $\mathcal{P}_L^{B,U}$ to the pebble tree $\mu(T)$ of $\mathcal{P}_L^{B,U}$ obtained by a vertical symmetry of the tree, meaning that $\mu(T)$ is defined inductively by

https://doi.org/10.4153/S0008414X25000094 Published online by Cambridge University Press

- if $T$ is just a leaf, then $\mu(T)$ is just a leaf,
- if $T$ is a node with pebbles $P$ and children $C_1, \dots, C_j$, then $\mu(T)$ is a node with pebbles $P$ and children $\mu(C_j), \dots, \mu(C_1)$.

***Definition 2.3*** If $\gamma \in U$, the *$\gamma$-balancing map* sends a pebble tree $T$ of $\mathcal{P}_L^{B,U}$ to the pebble tree $\beta_\gamma(T)$ of $\mathcal{P}_L^{B\cup\{\gamma\},U\setminus\{\gamma\}}$ whose root has a single pebble of color $\gamma$ and a single child $T$.

***Definition 2.4*** If $\gamma \notin B \cup U$, the *$\gamma$-inserting map* sends a pebble tree $T$ of $\mathcal{P}_L^{B,U}$ to the pebble tree $\iota_\gamma(T)$ of $\mathcal{P}_L^{B\cup\{\gamma\},U}$ obtained from $T$ by replacing each leaf by a $\gamma$-leaf.

***Definition 2.5*** If $x \in L$ and $U = \varnothing$, the *$x$-rerooting map* sends a pebble tree $T$ of $\mathcal{P}_L^{B,\varnothing}$ to the pebble tree $\rho_x(T) \in \mathcal{P}_L^{B,\varnothing}$ obtained by hanging $T$ from its leaf $x$. In other words, $\rho_x(T)$ is the tree on the nodes of $T$ where the children of each node $p$ of $T$ are the neighbors $c$ of $p$ in $T$ so that $x$ is in the connected component of $p$ in the tree $T$ were we have deleted the edge joining $p$ to $c$.

***Definition 2.6*** If $\ell > 1$, $B = \varnothing$ and $\gamma \notin U$, the *$\gamma$-uprooting map* sends a pebble tree $T$ of $\mathcal{P}_{[\ell]}^{\varnothing,U}$ to the pebble tree $\theta_\gamma(T)$ of $\mathcal{P}_{[\ell-1]}^{U\cup\{\gamma\},\varnothing}$ obtained from $T$ by first hanging $T$ from its rightmost leaf, then deleting the leftmost leaf and placing a $\gamma$-pebble at its parent, and finally replacing all remaining leaves except the first by a $\gamma$-leaf.

Finally, our next three remarks connect pebble trees with other relevant families of trees.

***Remark 2.5*** Consider a word $\alpha \in \{\text{I}, \text{O}\}^{\ell+1}$ starting with O (here, I and O stand for incoming and outgoing). An *$\alpha$-tree* is a rooted oriented planar tree such that

- labeling the external arrows counterclockwise starting from the root, the $i$th arrow is incoming if $\alpha_i = \text{I}$ and outgoing if $\alpha_i = \text{O}$,
- each internal node has at least one outgoing arrow,
- there is no node with precisely one incoming and one outgoing arrow.

These trees arise in the combinatorics of algebras endowed with a binary product and a co-inner product. They are studied in details in [PT18]. It turns out that they can be understood from pebble trees.

First, as illustrated in Figure 4, there are simple bijections between the pebble trees of $\mathcal{P}_\ell^{1,0}$ and the $\text{O}^{\ell+1}$-trees (meaning the trees where all leaves are outgoing):

- Starting from a pebble tree $T \in \mathcal{P}_\ell^{1,0}$, orient each arc $(p, c)$ joining a parent $p$ to one of its children $c$ in $T$ from $c$ to $p$ if $c$ is balanced, and from $p$ to $c$ if $c$ is unbalanced, orient the root and leaves outward, and forget all pebbles.
- Starting from a $\text{O}^{\ell+1}$-tree, place at each node one less pebbles than its outdegree, and forget the orientations.

In the present paper, we prefer our interpretation as pebble trees as it enables us to consider several pebble colors simultaneously.

Consider now an arbitrary signature $\alpha$. Although not explicit in [PT18], there is a clear map from $\alpha$-trees to $\text{O}^{\ell+1}$-trees, which consists in replacing each incoming external arrow (like ) by a node with a pair of outgoing arrows (like ). This leads to a bijection between the $\alpha$-trees and the pebble trees of $\mathcal{P}_\ell^{1,0}$ where the parent of the $i$th leaf is a unary node marked with a pebble.

https://doi.org/10.4153/S0008414X25000094 Published online by Cambridge University Press

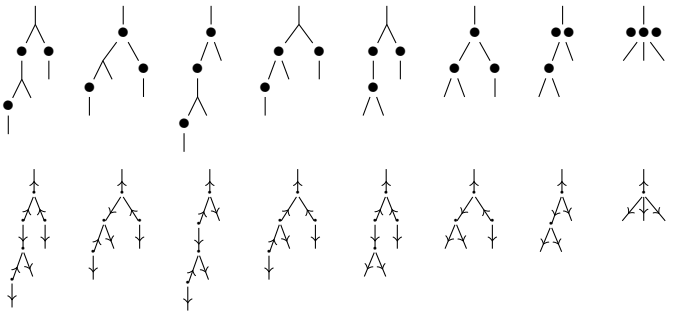


*Figure 4*: Examples of the bijection between the pebble trees of $\mathcal{P}_3^{1,0}$ and the $o^4$-trees.

***Remark 2.6*** The reader familiar with the bijective combinatorics of planar maps might also see some connections with the $\beta$-trees of [JS98, CS03]. Indeed, labeling each node $p$ of a pebble tree by the pebble default $\Delta_\gamma(T_p)$, we obtain a $\beta(1,1)$-tree. However, this map is clearly injective but not surjective, and the additional condition given by the pebble trees is unclear on $\beta(1,1)$-trees.

***Remark 2.7*** There is also a natural map from the pebble trees of $\mathcal{P}_\ell^{1,0}$ to the painted trees corresponding to the faces of the multiplihedron [Sta70, For08, CP22]. Namely, we can just forget all pebbles which have a pebble on the path to the root of the pebble tree to obtain a painted tree.

## 2.2 Pebble tree contraction poset

We now define the contraction poset on pebble trees, and will see that it is the face poset of a simplicial complex in Section 2.3 and of a polytope in Section 3.3.

***Definition 2.7*** For any node $c$ (not a leaf, nor the root) with parent $p$ in a pebble tree $T$, the *contraction* of $c$ in $T$ is the pebble tree $T/c$ obtained by replacing $c$ by its children in the list of children of $p$ and adding to $p$ the pebbles of $c$. The *pebble tree contraction poset* $\mathcal{PP}_\ell^{b,u}$ is the poset of contractions on pebble trees of $\mathcal{P}_\ell^{b,u}$.

***Example 2.8*** In the extreme situations of Example 2.1:

- the pebble tree contraction poset $\mathcal{PP}_1^{b,u}$ is the refinement poset on ordered partitions of $[b]$,
- the pebble tree contraction poset $\mathcal{PP}_\ell^{0,0}$ is the contraction poset on Schröder trees with $\ell$ leaves.

The pebble tree contraction posets $\mathcal{PP}_3^{0,1}$ and $\mathcal{PP}_2^{1,1}$ are illustrated in Figures 5 and 6. The fact that $\mathcal{PP}_3^{0,1}$ and $\mathcal{PP}_2^{1,1}$ are isomorphic can be seen applying successively Points (5), (4), and (2) of Proposition 2.10 below.

***Remark 2.9*** Observe that:

- The set of pebble trees $\mathcal{P}_\ell^{b,u}$ is clearly closed under contraction. Hence, the pebble tree contraction poset is a simplicial poset (a poset where each interval is a boolean algebra).

https://doi.org/10.4153/S0008414X25000094 Published online by Cambridge University Press

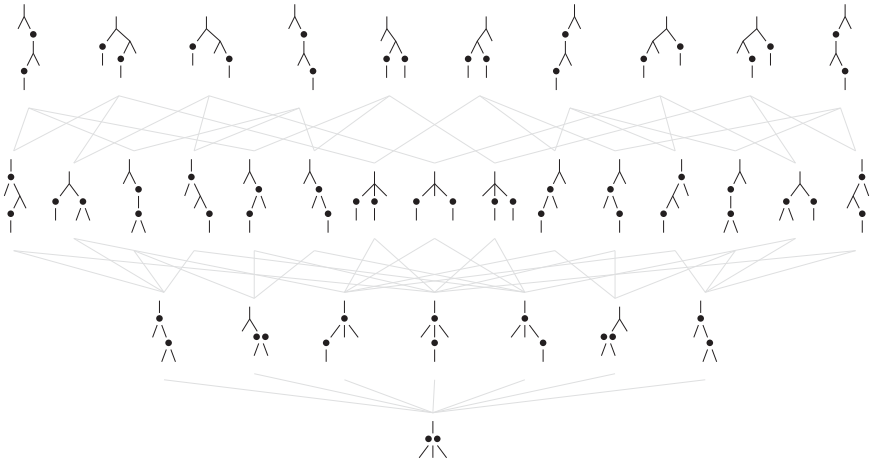


*Figure 5*: The pebble tree contraction poset $\mathcal{PP}_3^{0,1}$.

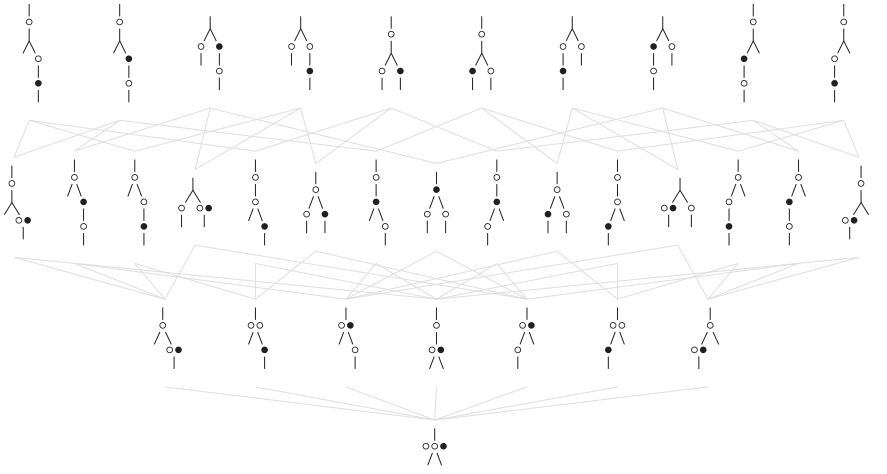


*Figure 6*: The pebble tree contraction poset $\mathcal{PP}_2^{1,1}$.

- The pebble tree contraction poset is ranked: the rank of a pebble tree is its number of nodes.
- The *maximal* pebble trees of $\mathcal{PP}_\ell^{b,u}$ are the pebble trees with only unary nodes containing a single pebble and binary nodes containing no pebble (hence, they have $\ell(b+u)-u$ unary nodes and $\ell-1$ binary nodes, thus rank $\ell(1+b+u)-u-1$).
- The *minimal* pebble tree of $\mathcal{PP}_\ell^{b,u}$ is the corolla with $\ell$ leaves and $\ell(b+u)-u$ pebbles at the root (hence it has rank 1).

Observe now that the mirroring, balancing, inserting, rerooting and uprooting maps of Definitions 2.2–2.6 obviously commute with contractions. This implies the following statement.

https://doi.org/10.4153/S0008414X25000094 Published online by Cambridge University Press

***Proposition 2.10*** *Consider the operations of Definitions 2.2–2.6.*

(1) *The mirroring map of Definition 2.2 defines a poset automorphism of* $\mathcal{PP}_\ell^{b,u}$.
(2) *If* $u > 1$, *the balancing map of Definition 2.3 defines a poset isomorphism from the pebble tree contraction poset* $\mathcal{PP}_\ell^{b,u}$ *to a principal upper set of the pebble tree contraction poset* $\mathcal{PP}_\ell^{b+1,u-1}$. *Hence,* $\mathcal{PP}_\ell^{b,u}$ *is isomorphic to a principal upper set of* $\mathcal{PP}_\ell^{b+u,0}$.
(3) *The inserting map of Definition 2.4 defines a poset isomorphism from the pebble tree contraction poset* $\mathcal{PP}_\ell^{b,u}$ *to a principal upper set of the pebble tree contraction poset* $\mathcal{PP}_\ell^{b+1,u}$.
(4) *The rerooting maps of Definition 2.5 define poset automorphisms of* $\mathcal{PP}_\ell^{b,0}$.
(5) *If* $\ell > 1$, *the uprooting map of Definition 2.6 defines a poset isomorphism from the pebble tree contraction poset* $\mathcal{PP}_\ell^{0,u}$ *to a principal upper set of the pebble tree contraction poset* $\mathcal{PP}_{\ell-1}^{u+1,0}$.

Finally, we connect the $\alpha$-trees of [PT18] to an upper set of the pebble tree contraction poset.

***Remark 2.11*** Following Remark 2.5, observe that for any signature $\alpha \in \mathrm{o} \cdot \{\mathrm{i}, \mathrm{o}\}^\ell$, the $\alpha$-tree contraction poset is isomorphic to the principal upper set of the pebble tree contraction poset $\mathcal{PP}_\ell^{1,0}$ generated by the pebble tree whose root has $\ell - |\alpha|_\mathrm{i}$ pebbles and $\ell$ children, and whose $i$th children is a leaf if $\alpha_i = \mathrm{o}$ and a unary node with one pebble and a leaf if $\alpha_i = \mathrm{i}$.

***Remark 2.12*** The following observations are consequences of Remarks 2.5 and 2.11 and Proposition 2.10:

- the $\mathrm{o}^{\ell+1}$-tree contraction poset is isomorphic to the pebble tree contraction poset $\mathcal{PP}_\ell^{1,0}$,
- for any $\alpha \in \mathrm{o} \cdot \{\mathrm{i}, \mathrm{o}\}^\ell$ with a single occurrence of i, the $\alpha$-tree contraction poset is isomorphic to the pebble tree contraction poset $\mathcal{PP}_\ell^{0,1}$,
- for $\alpha = \mathrm{oo}\mathrm{i}^{\ell-1}$ or $\alpha = \mathrm{o}\mathrm{i}^{\ell-1}\mathrm{o}$, the $\alpha$-tree contraction poset is isomorphic to the pebble tree contraction poset $\mathcal{PP}_{\ell+1}^{0,0}$ (*i.e.,* the contraction poset on Schröder trees).

## 2.3 Pebble tree complex

As mentioned in Remark 2.9, the pebble tree contraction poset $\mathcal{PP}_\ell^{b,u}$ is a simplicial poset. We now construct the corresponding simplicial complex. For a pebble tree in $\mathcal{PP}_\ell^{b,u}$, recall that we label the leaves by $[\ell]$ from left to right, the balanced pebble colors by $[b]$, and the unbalanced pebble colors by $[b+1, b+u]$. Recall also that we denote by $\mathsf{L}(S)$ and $\mathsf{B}(S)$ the sets of leaves and of balanced colors in a subtree $S$. We will moreover need the following notation and definition, which might be mysterious at first sight, but aims at generalizing Example 2.14 and will be crucial in Section 3.2.

***Notation 2.13*** *For an interval* $L := [s, t] \subseteq [\ell]$ *and a subset* $B \subseteq [b+u]$, *we define the sets*

$$L \otimes B := \bigcup_{p \in B} [\ell p + s - 1, \ell p + t - 1] \qquad \text{and} \qquad L \boxtimes B := [s, t-1] \cup (L \otimes B).$$

***Definition 2.8*** The *pebble tree complex* $\mathcal{PC}_\ell^{b,u}$ is the simplicial complex whose simplices are the sets $\Lambda(T) := \{\lambda(S) \mid S \text{ subtree of } T\}$ for all pebble trees $T \in \mathcal{P}_\ell^{b,u}$, where $\lambda(S) := \mathsf{L}(S) \boxtimes \mathsf{B}(S)$.

https://doi.org/10.4153/S0008414X25000094 Published online by Cambridge University Press

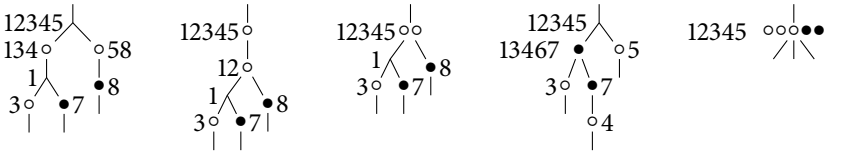



*Figure 7*: Some ∘-balanced and •-unbalanced $\{\circ,\bullet\}$-pebble trees $T$ and the associated simplices $\Lambda(T)$. Each node $n$ of $T$ is labeled by the concatenation of the elements of the set $\lambda(T_n)$.

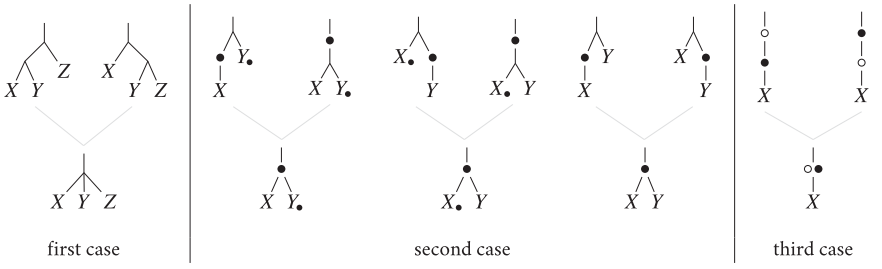



*Figure 8*: The pebble tree complex is a pseudomanifold. All possible corank 1 pebble trees are obtained by contracting precisely two maximal pebble trees. In the second (resp. third) picture, we mark $Y$ (resp. $X$) with a • to indicate that it is •-balanced. Neither $X$ nor $Y$ are •-balanced in the fourth picture.

***Example 2.14*** In the extreme situations of Example 2.1:

- the simplices of the pebble tree complex $\mathcal{PC}_1^{b,u}$ are the flags $B_1 \subsetneq B_2 \subsetneq \cdots \subsetneq B_k \subseteq [b]$,
- the simplices of the pebble tree complex $\mathcal{PP}_\ell^{0,0}$ are the collections of pairwise nested or non-adjacents intervals of $[\ell-1]$.

Figure 7 illustrates some more generic examples of simplices $\Lambda(T)$. Note that in these trees, the white color ∘ is labeled 1 while the black color • is labeled 2.

***Proposition 2.15*** *The pebble tree complex $\mathcal{PC}_\ell^{b,u}$ is a pseudomanifold, whose face poset is isomorphic to the pebble tree poset $\mathcal{PP}_\ell^{b,u}$.*

**Proof** Observe first that $\Lambda(T/n) = \Lambda(T)\backslash\{\lambda(T_n)\}$ for any node $n$ (not a leaf, nor the root) in a pebble tree $T$. Hence, the face poset of $\mathcal{PC}_\ell^{b,u}$ is indeed isomorphic to $\mathcal{PP}_\ell^{b,u}$. We thus obtain that $\mathcal{PC}_\ell^{b,u}$ is a pure simplicial complex since $\mathcal{PP}_\ell^{b,u}$ is a ranked simplicial poset. It remains to prove that $\mathcal{PC}_\ell^{b,u}$ is a pseudomanifold, meaning that any ridge (*i.e.,* codimension 1 face) is contained in precisely two facets (*i.e.,* maximal dimensional faces). Consider thus a pebble tree of corank 1, and let $p$ be the only node which is neither unary with a pebble, nor binary with no pebble. We want to prove that there are two ways to open $p$, meaning to replace $p$ by an edge whose contraction gives back $p$. We distinguish three cases:

- If $p$ has three children and no pebble, then there are two ways to open $p$ as usual (see Figure 8 (left)) and it does not matter whether $p$ and its children are balanced or not for each pebble color.

https://doi.org/10.4153/S0008414X25000094 Published online by Cambridge University Press

- If $p$ has two children and a $\gamma$-pebble, then $p$ is $\gamma$-balanced, and there are still two ways to open $p$ depending on whether its children are $\gamma$-balanced or not (see Figure 8 (middle)).
- If $p$ has one child and two pebbles of different colors, then there are still two ways to open $p$ choosing which pebble goes in the parent and which pebble goes in the child (see Figure 8 (right)).

■

***Remark 2.16*** In contrast to the special situations of Example 2.1, the pebble tree complex is not flag in general. For instance, $\mathcal{PC}_2^{1,0}$ and $\mathcal{PC}_3^{0,1}$ are not flag.

Finally, we translate Proposition 2.10 and Remark 2.11 to the pebble tree complex.

***Proposition 2.17*** *Consider the operations of Definitions 2.2–2.6.*

(1) *The map defined by* $\ell j + i - \delta_{j\neq 0} \mapsto \ell(j+1) - i$ *for any* $(i,j) \in ([\ell] \times [0, b+u]) \backslash \{(\ell, 0)\}$ *induces an automorphism of the pebble tree complex* $\mathcal{PC}_\ell^{b,u}$.
(2) *If* $u > 1$, *the pebble tree complex* $\mathcal{PC}_\ell^{b,u}$ *is isomorphic to the link of the face* $[\ell] \boxtimes [b]$ *in the pebble tree complex* $\mathcal{PC}_\ell^{b+1,u-1}$. *Hence,* $\mathcal{PC}_\ell^{b,u}$ *is isomorphic to a link of* $\mathcal{PC}_\ell^{b+u,0}$.
(3) *The pebble tree complex* $\mathcal{PC}_\ell^{b,u}$ *is isomorphic to the link of the face* $\{\{i\} \boxtimes [1] \mid i \in [\ell]\}$ *in the pebble tree complex* $\mathcal{PC}_\ell^{b+1,u}$.
(4) *The rerooting maps of Definition 2.5 induce automorphisms of the pebble tree complex* $\mathcal{PC}_\ell^{b,0}$.
(5) *If* $\ell > 1$, *the pebble tree complex* $\mathcal{PC}_\ell^{0,u}$ *is isomorphic to the link of the face* $\{\{i\} \boxtimes [1] \mid i \in [2, \ell-1]\}$ *in the pebble tree complex* $\mathcal{PC}_{\ell-1}^{u+1,0}$.

***Remark 2.18*** Following Remarks 2.5 and 2.11, observe that for any signature $\alpha \in \{1,0\}^{\ell+1}$, the $\alpha$-tree complex is isomorphic to the link of the face $\{\{i\} \boxtimes [1] \mid \alpha_i = 1\}$ in the pebble tree complex $\mathcal{PC}_\ell^{1,0}$.

## 2.4 Pebble tree flip graph

As the pebble tree complex $\mathcal{PC}_\ell^{b,u}$ is a pseudomanifold by Proposition 2.15, it is natural to consider its dual graph.

***Definition 2.9*** Two maximal pebble trees $T$ and $T'$ of $\mathcal{PP}_\ell^{b,u}$ are related by a *flip* if there are nodes $n$ of $T$ and $n'$ of $T'$ such that the following equivalent conditions hold:

- the contraction $T/n$ coincides with the contraction $T'/n'$,
- $\Lambda(T) \backslash \{\lambda(T_n)\} = \Lambda(T') \backslash \{\lambda(T'_{n'})\}$.

All possible types of flips are illustrated in Figure 9. The *flip graph* is the graph whose vertices are the maximal pebble trees of $\mathcal{PP}_\ell^{b,u}$ and whose edges are the flips between them.

***Example 2.19*** In the extreme situations of Example 2.1:

- the flip graph on $\mathcal{P}_1^{b,u}$ is the graph of adjacent transpositions on permutations of $[b]$,
- the flip graph on $\mathcal{P}_\ell^{0,0}$ is the rotation graph on binary trees with $\ell$ leaves.

https://doi.org/10.4153/S0008414X25000094 Published online by Cambridge University Press

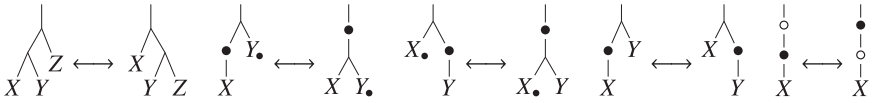



*Figure 9*: All possible flips in a maximal pebble tree. In the second (resp. third) picture, we mark $Y$ (resp. $X$) with a $\bullet$ to indicate that it is $\bullet$-balanced. Neither $X$ nor $Y$ are $\bullet$-balanced in the fourth picture.

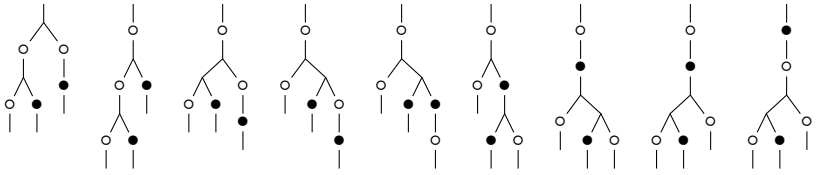


*Figure 10*: A sequence of flips in maximal $\circ$-balanced and $\bullet$-unbalanced $\{\circ,\bullet\}$-pebble trees.

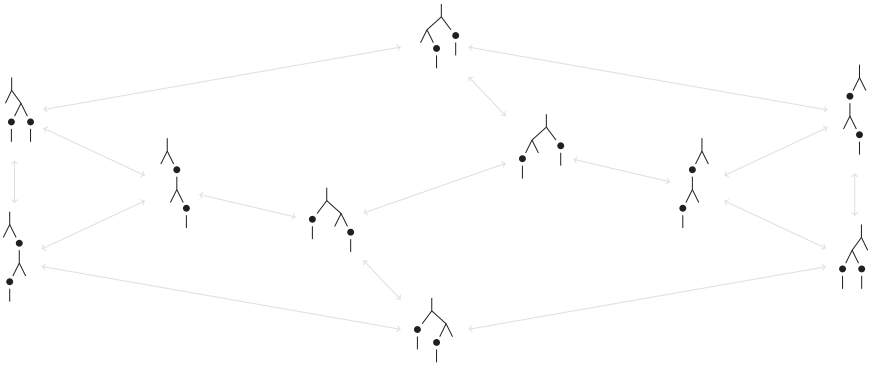


*Figure 11*: The flip graph on pebble trees of $\mathcal{P}_3^{0,1}$.

These extreme situations correspond to the right and left cases of Figure 9 respectively. Figure 10 illustrates a sequence of flips in maximal pebble trees of $\mathcal{P}_3^{1,1}$. Figures 11 and 12 illustrate the flip graphs on maximal pebble trees of $\mathcal{P}_3^{0,1}$ and $\mathcal{P}_2^{1,1}$ (which are isomorphic by Proposition 2.10 as already mentioned before).

As the dual graph of a pure simplicial pseudomanifold, the pebble tree flip graph is regular. Its degree is $\ell(1+b+u)-u-2$. As we will see in Theorem 3.8 that it is the graph of a simple polytope, it has the connectivity of its degree. Among various further properties of this graph that would require more investigations, we mention the following problem in connection to [STT88, Pou14].

***Problem 2.20*** *Evaluate the diameter of the flip graph on maximal pebble trees of* $\mathcal{P}_\ell^{b,u}$.

Finally, note that Proposition 2.10 and Remark 2.11 directly translate to morphisms between the flip graphs on the corresponding trees.

https://doi.org/10.4153/S0008414X25000094 Published online by Cambridge University Press

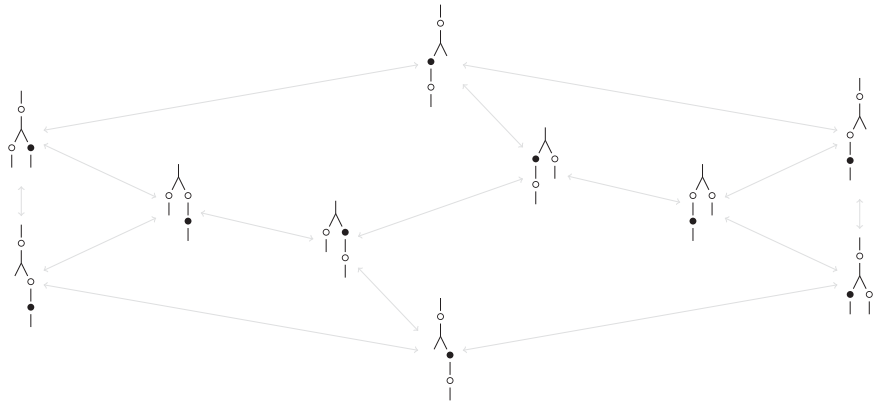


*Figure 12*: The flip graph on pebble trees of $\mathcal{P}_2^{1,1}$.

## 3 Pebble tree geometry

This section is devoted to the geometry of pebble trees. After quickly reminding the reader some geometric preliminaries (Section 3.1), we construct the pebble tree fan (Section 3.2) and the pebble tree polytope (Section 3.3).

### 3.1 Geometric preliminaries

We refer to [Zie98] for a reference on polyhedral geometry, and only remind the basic notions needed later in the paper.

A (polyhedral) *cone* is the positive span $\mathbb{R}_{\geq 0}\boldsymbol{R}$ of a finite set $\boldsymbol{R}$ of vectors of $\mathbb{R}^d$ or equivalently, the intersection of finitely many closed linear half-spaces of $\mathbb{R}^d$. The *faces* of a cone are its intersections with its supporting hyperplanes. The *rays* (resp. *facets*) are the faces of dimension 1 (resp. codimension 1). A cone is *simplicial* if its rays are linearly independent. A (polyhedral) *fan* $\mathcal{F}$ is a set of cones such that any face of a cone of $\mathcal{F}$ belongs to $\mathcal{F}$, and any two cones of $\mathcal{F}$ intersect along a face of both. A fan is *essential* if the intersection of its cones is the origin, *complete* if the union of its cones covers $\mathbb{R}^d$, and *simplicial* if all its cones are simplicial.

Note that a simplicial fan defines a simplicial complex on its rays (the simplices of the simplicial complex are the subsets of rays which span a cone of the fan). Conversely, given a simplicial complex $\Delta$ with ground set $V$, one can try to realize it geometrically by associating a ray $\boldsymbol{r}_v$ of $\mathbb{R}^d$ to each $v \in V$, and the cone $\mathbb{R}_{\geq 0}\boldsymbol{R}_\triangle$ generated by the set $\boldsymbol{R}_\triangle := \{\boldsymbol{r}_v \mid v \in \triangle\}$ to each $\triangle \in \Delta$. To show that the resulting cones indeed form a fan, we will need the following statement, which can be seen as a reformulation of [DRS10, Corollary 4.5.20].

***Proposition 3.1*** *Consider a closed simplicial pseudomanifold $\Delta$ with ground set $V$ and a set of vectors $(\boldsymbol{r}_v)_{v\in V}$ of $\mathbb{R}^d$, and define $\boldsymbol{R}_\triangle := \{\boldsymbol{r}_v \mid v \in \triangle\}$ for any $\triangle \in \Delta$. Then the collection of cones $\{\mathbb{R}_{\geq 0}\boldsymbol{R}_\triangle \mid \triangle \in \Delta\}$ forms a complete simplicial fan of $\mathbb{R}^d$ if and only if*

https://doi.org/10.4153/S0008414X25000094 Published online by Cambridge University Press

- *there exists a vector* $\boldsymbol{v}$ *of* $\mathbb{R}^d$ *contained in only one of the open cones* $\mathbb{R}_{>0}\boldsymbol{R}_\triangle$ *for* $\triangle \in \Delta$,
- *for any two adjacent facets* $\triangle, \triangle'$ *of* $\Delta$ *with* $\triangle\backslash\{v\} = \triangle'\backslash\{v'\}$, *we have* $\alpha_v\alpha_{v'} > 0$ *where*

$$\alpha_v \boldsymbol{r}_v + \alpha_{v'} \boldsymbol{r}_{v'} + \sum_{w\in\triangle\cap\triangle'} \alpha_w \boldsymbol{r}_w = 0$$

*denotes the unique (up to rescaling) linear dependence on* $\boldsymbol{R}_{\triangle\cup\triangle'}$.

A *polytope* is the convex hull of finitely many points of $\mathbb{R}^d$ or equivalently, a bounded intersection of finitely many closed affine half-spaces of $\mathbb{R}^d$. The *faces* of a polytope are its intersections with its supporting hyperplanes. The *vertices* (resp. *edges*, resp. *facets*) are the faces of dimension 0 (resp. dimension 1, resp. codimension 1).

The *normal cone* of a face $\mathbb{F}$ of a polytope $\mathbb{P}$ is the cone generated by the normal vectors to the supporting hyperplanes of $\mathbb{P}$ containing $\mathbb{F}$. Said differently, it is the cone of vectors $\boldsymbol{c}$ of $\mathbb{R}^d$ such that the linear form $\boldsymbol{x} \mapsto \langle \boldsymbol{c} \mid \boldsymbol{x} \rangle$ on $\mathbb{P}$ is maximized by all points of the face $\mathbb{F}$. The *normal fan* of $\mathbb{P}$ is the set of normal cones of all its faces.

Consider now a complete simplicial fan $\mathcal{F}$ of $\mathbb{R}^d$ with rays $(\boldsymbol{r}_v)_{v\in V}$ and cones $\mathbb{R}_{\geq 0}\boldsymbol{R}_\triangle$ for $\triangle \in \Delta$, where $\boldsymbol{R}_\triangle := \{\boldsymbol{r}_v \mid v \in \triangle\}$ as in Proposition 3.1. To realize the fan $\mathcal{F}$, one can try to pick a height vector $\boldsymbol{h} := (h_v)_{v\in V} \in \mathbb{R}^V$ and consider the polytope $\mathbb{P}_{\boldsymbol{h}} := \{\boldsymbol{x}\in\mathbb{R}^d \mid \langle \boldsymbol{r}v \mid \boldsymbol{x} \rangle \leq h_v \text{ for all } v\in V\}$. The following classical statement characterizes the height vectors $\boldsymbol{h}$ for which the fan $\mathcal{F}$ is the normal fan of this polytope $\mathbb{P}_{\boldsymbol{h}}$. We borrow the formulation from [CFZ02, Lemma 2.1].

***Proposition 3.2*** *Let* $\mathcal{F}$ *be an essential complete simplicial fan in* $\mathbb{R}^n$ *with rays* $(\boldsymbol{r}_v)_{v\in V}$ *and cones* $\mathbb{R}_{\geq 0}\boldsymbol{R}_\triangle$ *for* $\triangle \in \Delta$. *Then the following are equivalent for any height vector* $\boldsymbol{h} \in \mathbb{R}^V$:

- *The fan* $\mathcal{F}$ *is the normal fan of the polytope*

$$\mathbb{P}_{\boldsymbol{h}} := \left\{\boldsymbol{x} \in \mathbb{R}^d \;\middle|\; \langle \boldsymbol{r}_v \mid \boldsymbol{x} \rangle \leq h_v \text{ for all } v \in V\right\}.$$

- *For two adjacent facets* $\triangle, \triangle'$ *of* $\Delta$ *with* $\triangle\backslash\{v\} = \triangle'\backslash\{v'\}$, *the height vector* $\boldsymbol{h}$ *satisfies the wall crossing inequality*

$$\alpha_v h_v + \alpha_{v'} h_{v'} + \sum_{w\in\triangle\cap\triangle'} \alpha_w h_w > 0$$

*where*

$$\alpha_v \boldsymbol{r}_v + \alpha v' \boldsymbol{r}_{v'} + \sum_{w\in\triangle\cap\triangle'} \alpha_w \boldsymbol{r}_w = 0$$

*denotes the unique linear dependence on* $\boldsymbol{R}_{\triangle\cup\triangle'}$ *such that* $\alpha_v + \alpha_{v'} = 2$.

## 3.2 Pebble tree fan

Fix $\ell, b, u \in \mathbb{N}$ and consider the intervals

$$I_0 := [\ell(b+1) - 1] \qquad \text{and} \qquad I_i := [\ell(b+i), \ell(b+i+1) - 1] \quad \text{for all } i \in [u]$$

whose union is the interval

$$I := I_0 \sqcup I_1 \sqcup \cdots \sqcup I_u = [\ell(b+u+1) - 1].$$

https://doi.org/10.4153/S0008414X25000094 Published online by Cambridge University Press

We work in the Euclidean space $\mathbb{R}^I$ with canonical basis $(\boldsymbol{e}_i)_{i\in I}$. We denote by $\mathbf{1}_J := \sum_{j\in J} \boldsymbol{e}_j$ the characteristic vector of a subset $J \subseteq I$. As our constructions actually live in the linear subspace

$$\mathbb{H}_\ell^{b,u} := \left\{ \boldsymbol{x} \in \mathbb{R}^I \;\middle|\; \langle\, \mathbf{1}_{I_i} \mid \boldsymbol{x} \,\rangle = 0 \text{ for all } 0 \le i \le u \right\},$$

we define the vector

$$\boldsymbol{r}_J := \sum_{i=0}^{u} \left( |I_i \backslash J| \cdot \mathbf{1}_{I_i \cap J} - |I_i \cap J| \cdot \mathbf{1}_{I_i \backslash J} \right) \in \mathbb{H}_\ell^{b,u}$$

for each subset $J \subseteq I$. It is immediate to check that these vectors satisfy the linear dependences

$$\boldsymbol{r}_J + \boldsymbol{r}_K = \boldsymbol{r}_{J\cup K} + \boldsymbol{r}_{J\cap K}$$

for any $J, K \subseteq I$. Finally, we associate to any pebble subtree $S$ the vector $\boldsymbol{r}_S := \boldsymbol{r}_{\lambda(S)} = \boldsymbol{r}_{\mathsf{L}(S)\boxtimes\mathsf{B}(S)}$ where $\mathsf{L}(S)$ and $\mathsf{B}(S)$ denote the sets of leaves and of balanced colors in $S$, and the operation $\boxtimes$ was defined in Definition 2.13. Note that $\boldsymbol{r}_S = \mathbf{0}$ when $S$ is the entire tree $T$ (because $\mathsf{L}(T) = [\ell]$ and $\mathsf{B}(T) = [b]$ so that $\lambda(T) = I_0$) or when $S$ is a leaf $i$ (because $\mathsf{L}(S) = \{i\}$ and $\mathsf{B}(S) = \varnothing$ so that $\lambda(S) = \varnothing$). We now use these vectors $\boldsymbol{r}_S$ to construct the pebble tree fan.

***Definition 3.1*** The *pebble tree fan* $\mathcal{PF}_\ell^{b,u}$ is the collection of cones

$$\mathbb{C}(T) := \operatorname{cone}\{\boldsymbol{r}_S \mid S \text{ subtree of } T\}$$

for all pebble trees $T \in \mathcal{P}_\ell^{b,u}$, where $\boldsymbol{r}_S := \boldsymbol{r}_{\lambda(S)} = \boldsymbol{r}_{\mathsf{L}(S)\boxtimes\mathsf{B}(S)}$.

***Example 3.3*** In the extreme situations of Example 2.1:

- the pebble tree fan $\mathcal{PF}_1^{b,u}$ is the braid fan, with a ray $\boldsymbol{r}_J$ for each proper subset $\varnothing \neq J \subsetneq [b]$ and a maximal cone $\mathbb{C}(\sigma)$ for each permutation $\sigma$ of $[b]$, defined by the inequalities $x_{\sigma(1)} \le \cdots \le x_{\sigma(b)}$,
- the pebble tree fan $\mathcal{PF}_\ell^{0,0}$ is the sylvester fan, with a ray $\boldsymbol{r}_J$ for each proper interval $J$ of $[\ell]$ and a maximal cone $\mathbb{C}(T)$ for each binary tree $T$, defined by the inequalities $x_i \le x_j$ whenever there is a path from $i$ to $j$ in the tree $T$ labeled in inorder and oriented toward its root.

Note that the sylvester fan coarsens the braid fan: the cone $\mathbb{C}(T)$ of the sylvester fan can also be obtained by glueing the cones $\mathbb{C}(\sigma)$ of the braid fan corresponding to the linear extensions $\sigma$ of $T$.

***Theorem 3.4*** *The pebble tree fan $\mathcal{PF}_\ell^{b,u}$ is an essential complete simplicial fan in $\mathbb{H}_\ell^{b,u}$, whose face lattice is the pebble tree contraction poset $\mathcal{PP}_\ell^{b,u}$.*

The proof of Theorem 3.4 relies on the description of the linear dependences among adjacent maximal cones described in Lemma 3.6. To obtain these dependences, we need the following preliminary statement, where we use the operation $\otimes$ defined in Definition 2.13.

***Lemma 3.5*** *For any maximal pebble tree $S$ and any $B \subseteq \mathsf{B}(S)$, there are in $S$ some distinct unary subtrees $U_1, \dots, U_k$ with children $V_1, \dots, V_k$ respectively such that $\boldsymbol{r}_{\mathsf{L}(S)\otimes B} = \sum_{i\in[k]} \boldsymbol{r}_{U_i} - \boldsymbol{r}_{V_i}$.*

https://doi.org/10.4153/S0008414X25000094 Published online by Cambridge University Press

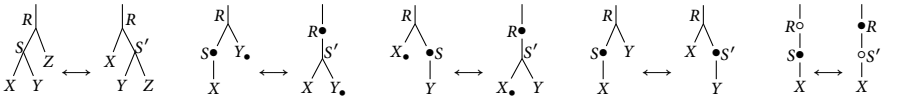


*Figure 13*: The four cases of the proof of 3.6.

**Proof** If a subtree $U$ has a $\gamma$-pebble and a unique child $V$, then we have $\boldsymbol{r}_{\mathsf{L}(U)\otimes\{\gamma\}} = \boldsymbol{r}_U - \boldsymbol{r}_V$ because $\mathsf{L}(U) = \mathsf{L}(V)$ and $\mathsf{B}(U) = \mathsf{B}(V) \sqcup \{\gamma\}$. Hence, for any $\gamma \in \mathsf{B}(S)$, if we denote by $U_1, \dots, U_k$ the closest descendants of $S$ with a $\gamma$-pebble and by $V_1, \dots, V_k$ their respective children, then we have $\boldsymbol{r}_{\mathsf{L}(S)\otimes\{\gamma\}} = \sum_{i\in[k]} \boldsymbol{r}_{\mathsf{L}(U_i)\otimes\{\gamma\}} = \sum_{i\in[k]} \boldsymbol{r}_{U_i} - \boldsymbol{r}_{V_i}$ because $\mathsf{L}(S) = \bigsqcup_{i\in[k]} \mathsf{L}(U_i)$. The result follows since $\boldsymbol{r}_{\mathsf{L}(S)\otimes B} = \sum_{\gamma\in B} \boldsymbol{r}_{\mathsf{L}(S)\otimes\{\gamma\}}$. ■

***Lemma 3.6*** *Let $T$ and $T'$ be two adjacent maximal pebble trees and let $S$ and $S'$ be the subtrees of $T$ and $T'$ such that $\Lambda(T)\backslash\{\lambda(S)\} = \Lambda(T')\backslash\{\lambda(S')\}$. Then there is a linear dependence among the rays $\boldsymbol{r}_R$ associated with the subtrees $R$ of $T$ and $T'$ where the rays $\boldsymbol{r}_S$ and $\boldsymbol{r}_{S'}$ both have coefficient* 1.

**Proof** We analyse the five possible types of flips described in Figure 9. In all cases, we denote by $R$ the parent of $S$ and $S'$. See Figure 13 here.

**Case 1.** For the first flip of Figure 13, we have

$$\mathsf{L}(S) = \mathsf{L}(X) \sqcup \mathsf{L}(Y) \quad \mathsf{L}(S') = \mathsf{L}(Y) \sqcup \mathsf{L}(Z) \quad \mathsf{L}(R) = \mathsf{L}(X) \sqcup \mathsf{L}(Y) \sqcup \mathsf{L}(Z)$$
$$\mathsf{B}(S) = \mathsf{B}(X) \cap \mathsf{B}(Y) \quad \mathsf{B}(S') = \mathsf{B}(Y) \cap \mathsf{B}(Z) \quad \mathsf{B}(R) = \mathsf{B}(X) \cap \mathsf{B}(Y) \cap \mathsf{B}(Z)$$

which yields

$$\boxed{\boldsymbol{r}_S + \boldsymbol{r}_{S'} = \boldsymbol{r}_R + \boldsymbol{r}_Y + \boldsymbol{r}_{\mathsf{L}(S)\otimes(\mathsf{B}(S)\backslash\mathsf{B}(R))} + \boldsymbol{r}_{\mathsf{L}(S')\otimes(\mathsf{B}(S')\backslash\mathsf{B}(R))} - \boldsymbol{r}_{\mathsf{L}(Y)\otimes\mathsf{B}(Y)}}$$

Since $\boldsymbol{r}_{\mathsf{L}(S)\otimes(\mathsf{B}(S)\backslash\mathsf{B}(R))}$ (resp. $\boldsymbol{r}_{\mathsf{L}(S')\otimes(\mathsf{B}(S')\backslash\mathsf{B}(R))}$, resp. $\boldsymbol{r}_{\mathsf{L}(Y)\otimes\mathsf{B}(Y)}$) is a linear combination of the rays $\boldsymbol{r}_P$ for some subtrees $P$ of $S$ distinct from $S$ (resp. of $S'$ distinct from $S'$, resp. of $Y$) by Lemma 3.5, this is indeed a linear dependence among the rays $\boldsymbol{r}_Q$ associated with the subtrees $Q$ of $T$ and $T'$ where the rays $\boldsymbol{r}_S$ and $\boldsymbol{r}_{S'}$ both have coefficient 1.

**Case 2.** For the second flip of Figure 13, we have

$$\mathsf{L}(S) = \mathsf{L}(X) \quad \mathsf{L}(S') = \mathsf{L}(X) \sqcup \mathsf{L}(Y) \quad \mathsf{L}(R) = \mathsf{L}(X) \sqcup \mathsf{L}(Y)$$
$$\mathsf{B}(S) = \mathsf{B}(X) \sqcup \{\bullet\} \quad \mathsf{B}(S') = \mathsf{B}(X) \cap \mathsf{B}(Y) \quad \mathsf{B}(R) = (\mathsf{B}(X) \cap \mathsf{B}(Y)) \sqcup \{\bullet\}$$

which yields $\boxed{\boldsymbol{r}_S + \boldsymbol{r}_{S'} = \boldsymbol{r}_R + \boldsymbol{r}_X - \boldsymbol{r}_{\mathsf{L}(Y)\otimes\{\bullet\}}}$

Again, we can develop $\boldsymbol{r}_{\mathsf{L}(Y)\otimes\{\bullet\}}$ using Lemma 3.5, so that we indeed obtained a linear dependence among the rays $\boldsymbol{r}_Q$ for the subtrees $Q$ of $T$ and $T'$ where the rays $\boldsymbol{r}_S$ and $\boldsymbol{r}_{S'}$ both have coefficient 1.

**Case 3.** The case of the third flip of Figure 13, is symmetric to Case 2.

https://doi.org/10.4153/S0008414X25000094 Published online by Cambridge University Press

**Case 4.** For the fourth flip of Figure 13, assume first that $R$ has an ancestor with a $\bullet$-pebble. Then we additionally denote

- by $U_0$ the closest ancestor of $R$ which has a $\bullet$-pebble,
- by $U_1, \dots, U_k$ the closest descendants of $U_0$ but not descendants of $R$ which have a $\bullet$-pebble,
- by $V_0, V_1, \dots, V_k$ the (unique) children of $U_0, U_1, \dots, U_k$ respectively.

We have

$$\begin{array}{lll} \mathsf{L}(S) = \mathsf{L}(X) & \mathsf{L}(S') = \mathsf{L}(Y) & \mathsf{L}(U_i) = \mathsf{L}(V_i) \\ \mathsf{B}(S) = \mathsf{B}(X) \sqcup \{\bullet\} & \mathsf{B}(S') = \mathsf{B}(Y) \sqcup \{\bullet\} & \mathsf{B}(U_i) = \mathsf{B}(V_i) \sqcup \{\bullet\} \end{array}$$

and moreover $\mathsf{L}(U_0) = \mathsf{L}(S) \sqcup \mathsf{L}(S') \sqcup \mathsf{L}(U_1) \sqcup \cdots \sqcup \mathsf{L}(U_k)$. Using Lemma 3.5, we get

$$\boldsymbol{r}_{U_0} - \boldsymbol{r}_{V_0} = \boldsymbol{r}_{\mathsf{L}(U_0)\otimes\{\bullet\}} = \boldsymbol{r}_S - \boldsymbol{r}_X + \boldsymbol{r}_{S'} - \boldsymbol{r}_Y + \boldsymbol{r}_{U_1} - \boldsymbol{r}_{V_1} + \cdots + \boldsymbol{r}_{U_k} - \boldsymbol{r}_{V_k}$$

or, written differently

$$\boxed{\boldsymbol{r}_S + \boldsymbol{r}_{S'} = \boldsymbol{r}_X + \boldsymbol{r}_Y + \boldsymbol{r}_{U_0} - \boldsymbol{r}_{V_0} - \boldsymbol{r}_{U_1} + \boldsymbol{r}_{V_1} + \cdots - \boldsymbol{r}_{U_k} + \boldsymbol{r}_{V_k}}$$

Now if $R$ has no ancestor with a $\bullet$-pebble, then using that $\boldsymbol{r}_{\mathsf{L}(T)\otimes\{\bullet\}} = \mathbf{0}$, we obtain similarly

$$\boxed{\boldsymbol{r}_S + \boldsymbol{r}_{S'} = \boldsymbol{r}_X + \boldsymbol{r}_Y - \boldsymbol{r}_{U_1} + \boldsymbol{r}_{V_1} + \cdots - \boldsymbol{r}_{U_k} + \boldsymbol{r}_{V_k}}$$

where

- $U_1, \dots, U_k$ are the closest descendants of the root of $T$ but not descendants of $R$ which have a $\bullet$-pebble,
- $V_1, \dots, V_k$ are the (unique) children of $U_1, \dots, U_k$ respectively.

**Case 5.** For the fifth flip of Figure 13, we have

$$\begin{array}{lll} \mathsf{L}(S) = \mathsf{L}(X) & \mathsf{L}(S') = \mathsf{L}(X) & \mathsf{L}(R) = \mathsf{L}(X) \\ \mathsf{B}(S) = \mathsf{B}(X) \sqcup \{\bullet\} & \mathsf{B}(S') = \mathsf{B}(X) \sqcup \{\circ\} & \mathsf{B}(R) = \mathsf{B}(X) \sqcup \{\circ, \bullet\} \end{array}$$

which yields $\boxed{\boldsymbol{r}_S + \boldsymbol{r}_{S'} = \boldsymbol{r}_R + \boldsymbol{r}_X}$

■

**Proof of Theorem 3.4** Note that $\mathcal{PF}_\ell^{b,u}$ is included in $\mathbb{H}_\ell^{b,u}$ since all rays $\boldsymbol{r}_{1=J}$ are. To prove that it is a complete simplicial fan, we just check the two criteria of Proposition 3.1. The second criterion is guaranteed by the description of the linear dependences in Lemma 3.6. For the first criterion, consider the vector

$$\boldsymbol{v} = \sum_{i\in[\ell-2]} \boldsymbol{r}_{[i]} + \sum_{i\in[b]} 2^{\ell+i} \boldsymbol{r}_{[\ell i, \ell(i+1)-1]} + \sum_{i\in[u]} 2^{\ell+b+i} \boldsymbol{r}_{[\ell i+1, \ell(i+1)-1]},$$

and a pebble tree $T$ such that $\boldsymbol{v}$ is contained in the interior of $\mathbb{C}(T)$. As the last $\ell-1$ coordinates of $\boldsymbol{v}$ are strictly larger than all other coordinates, each of the last $\ell-1$ leaves of $T$ is preceded by a unary node with pebble colored by $b+u$. Repeating the argument, we obtain that the first leaf of $T$ is preceded by a chain of unary nodes with pebbles colored $1, \dots, b$ while each of the last $\ell-1$ leaves if $T$ is preceded by a chain

https://doi.org/10.4153/S0008414X25000094 Published online by Cambridge University Press

of unary nodes with pebbles colored $1, \dots, b+u$. Finally, we obtain that the rest of the tree $T$ is the left comb since it is the only Schröder tree whose cone in the sylvester fan contains the vector $\sum_{i\in[\ell-2]} \boldsymbol{r}_{[i]}$. Finally, $\mathcal{PF}_\ell^{b,u}$ is essential as the dimension of its cones matches the dimension of $\mathbb{H}_\ell^{b,u}$. ■

***Remark 3.7*** A few observations on the pebble tree fan:

- The simple descriptions of Example 3.3 for the braid fan and for the sylvester fan unfortunately fail for arbitrary $b, u \geq 0$. Indeed, there is a natural way to label the nodes of a maximal pebble tree: label the binary nodes in inorder by $[\ell-1]$ and the unary nodes by the only leaf first covered by this pebble. This labeling yields a cone $\mathbb{C}(T)$ for each maximal pebble tree $T$, defined by $x_i \leq x_j$ whenever there is a directed path from $i$ to $j$ in the tree $T$ oriented toward its root. However, the cones $\mathbb{C}(T)$ for all maximal pebble trees $T$ do not define a complete simplicial fan (check out the case $\ell = 2$, $b = 1$ and $u = 0$). In fact, our pebble tree fan $\mathcal{PF}_\ell^{b,u}$ is not refined by the braid fan in general
- Our definition of the pebble tree fan $\mathcal{PF}_\ell^{b,u}$ respects some symmetries of the pebble tree complex $\mathcal{PC}_\ell^{b,u}$ but not all. See Proposition 3.11 for a precise statement directly on polytopes.
- Lemma 3.6 actually proves that the pebble tree fan $\mathcal{PF}_\ell^{b,u}$ is smooth, meaning that the principal vectors spanning the rays of any maximal cone of $\mathcal{PF}_\ell^{b,u}$ form an integral basis of the space (in other words, the corresponding toric variety is smooth).

## 3.3 Pebble tree polytope

Our next step is to construct a polytope whose normal fan is the pebble tree fan, using the criterion of Proposition 3.2.

***Definition 3.2*** A *submodular function* on $n$ is a map $f$ from the subsets of $[n]$ to $\mathbb{R}_{\geq 0}$ such that $f_\varnothing = 0$ and

$$f_{A\cup B} + f_{A\cap B} \leq f_A + f_B$$

for any subsets $A$ and $B$ of $[n]$. We then define

$$\Delta f := \min\left(f_A + f_B - f_{A\cup B} - f_{A\cap B}\right)$$

where the minimum ranges over all subsets $A$ and $B$ of $[n]$ such that $A \not\subseteq B$ and $A \not\supseteq B$. Note that

- $\sum_{i\in[k]} f_{A_i} - f_A \geq (k-1)\cdot\Delta f$ for any $A = \bigcup_{i\in[k]} A_i$ where $A_1, \dots, A_k$ are pairwise disjoint,
- $\Delta\lambda f = \lambda\Delta f$ for any scalar factor $\lambda$.

We say that $f$ is *strictly submodular* when $\Delta f > 0$.

***Theorem 3.8*** *Pick three strictly submodular functions $f$ on $\ell$, $g$ on $\ell$, and $h$ on $b+u$ such that*

$$\Delta f > 4(\ell b + \ell u - u)\cdot(\max g + \max h) \qquad \text{and} \qquad \Delta g > (\ell b + \ell u - u + 1)\cdot \max h.$$

https://doi.org/10.4153/S0008414X25000094 Published online by Cambridge University Press

*Then the pebble tree fan* $\mathcal{PF}_\ell^{b,u}$ *is the normal fan of the pebble tree polytope* $\mathbb{PTP}_\ell^{b,u}(f,g,h)$*, the* $(\ell+\ell b+\ell u-u-2)$*-dimensional polytope defined in the subspace* $\mathbb{H}_\ell^{b,u}$ *by the inequalities*

$$\left\langle \boldsymbol{r}_{[s,t]\boxtimes B} \,\middle|\, \boldsymbol{x} \right\rangle \le f_{[s,t]} + g_{[s,t]} \cdot |B| + h_B$$

*for all* $1 \le s \le t \le \ell$ *and all* $B \subseteq [b+u]$.

**Proof** To shorten notations in this proof, we define for a maximal pebble subtree $S$

$$f_S := f_{\mathsf{L}(S)}, \quad g_S := g_{\mathsf{L}(S)}, \quad h_S := h_{\mathsf{B}(S)}, \quad \text{and} \quad \varphi_S := f_{\mathsf{L}(S)} + g_{\mathsf{L}(S)} \cdot |\mathsf{B}(S)| + h_{\mathsf{B}(S)}.$$

Observe that if $V$ is the unique child of $U$, then $\varphi_U - \varphi_V = g_U + h_U - h_V$ because $\mathsf{L}(U) = \mathsf{L}(V)$ and $|\mathsf{B}(U)| = |\mathsf{B}(V)| + 1$. We just need to prove that the function $\varphi$ satisfies the wall-crossing inequalities of Proposition 3.2 for each of the linear dependences boxed in the proof of Lemma 3.6.

**Case 1.** By Lemmas 3.5 and 3.6, we have

$$\boldsymbol{r}_S + \boldsymbol{r}_{S'} - \boldsymbol{r}_R - \boldsymbol{r}_Y - \sum_{i\in[k]} (\boldsymbol{r}_{U_i} - \boldsymbol{r}_{V_i}) - \sum_{i\in[k']} (\boldsymbol{r}_{U'_i} - \boldsymbol{r}_{V'_i}) + \sum_{i\in[k'']} (\boldsymbol{r}_{U''_i} - \boldsymbol{r}_{V''_i}) = \boldsymbol{0}$$

for distinct unary subtrees $U_1, \dots, U_k$ of $S$ (resp. $U'_1, \dots, U'_{k'}$ of $S'$, resp. $U''_1, \dots, U''_{k''}$ of $Y$) with respective children $V_1, \dots, V_k$ (resp. $V'_1, \dots, V'_{k'}$, resp. $V''_1, \dots, V''_{k''}$). Since $\mathsf{L}(R) = \mathsf{L}(S) \cup \mathsf{L}(S')$ and $\mathsf{L}(Y) = \mathsf{L}(S) \cap \mathsf{L}(S')$, we have

$$\begin{aligned} f_S + f_{S'} - f_R - f_Y &\ge \Delta f > 4(\ell b + \ell u - u)(\max g + \max h) \\ &\ge (g_R + h_R) + (g_Y + h_Y) + \sum_{i\in[k]} (g_{U_i} + h_{U_i}) + \sum_{i\in[k']} (g_{U'_i} + h_{U'_i}) + \sum_{i\in[k'']} (g_{V''_i} + h_{V''_i}), \end{aligned}$$

where the last inequality holds since $U_i \ne U_j$ (resp. $U'_i \ne U'_j$, resp. $V''_i \ne V''_j$) for $i \ne j$, and the pebble tree $T$ has $\ell b + \ell u - u$ unary subtrees. Since $f, g, h$ take non-negative values and $\varphi_U - \varphi_V = g_U + h_U - h_V$ when $V$ is the unique child of $U$, we obtain that $\varphi$ satisfies the wall-crossing inequality

$$\varphi_S + \varphi_{S'} - \varphi_R - \varphi_Y - \sum_{i\in[k]} (\varphi_{U_i} - \varphi_{V_i}) - \sum_{i\in[k']} (\varphi_{U'_i} - \varphi_{V'_i}) + \sum_{i\in[k'']} (\varphi_{U''_i} - \varphi_{V''_i}) > 0.$$

**Case 2.** By Lemma 3.6, we have

$$(\boldsymbol{r}_R - \boldsymbol{r}_{S'}) - (\boldsymbol{r}_S - \boldsymbol{r}_X) - \sum_{i\in[k]} (\boldsymbol{r}_{U_i} - \boldsymbol{r}_{V_i}) = \boldsymbol{0}$$

for distinct unary subtrees $U_1, \dots, U_k$ of $Y$ with children $V_1, \dots, V_k$, such that $\bigsqcup_{i\in[k]} \mathsf{L}(U_i) = \mathsf{L}(Y)$. Since $\mathsf{L}(R) = \mathsf{L}(S) \sqcup \mathsf{L}(Y)$, we obtain that

https://doi.org/10.4153/S0008414X25000094 Published online by Cambridge University Press

$$g_R - g_S - \sum_{i\in[k]} g_{U_i} \geq (k-1)\cdot\Delta g \geq \Delta g > (\ell b + \ell u - u + 1)\cdot \max h \geq h_{S'} + h_S + \sum_{i\in[k]} h_{U_i},$$

where the last inequality holds since $S \neq U_i \neq U_j$ for $i \neq j$, and the subtree $R$ has at most $\ell b + \ell u - u$ unary subtrees. Since $f, g, h$ take non-negative values and $\varphi_U - \varphi_V = g_U + h_U - h_V$ when $V$ is the unique child of $U$, we obtain that $\varphi$ satisfies the wall-crossing inequality

$$(\varphi_R - \varphi_{S'}) - (\varphi_S - \varphi_X) - \sum_{i\in[k]} (\varphi_{U_i} - \varphi_{V_i}) > 0.$$

**Case 3.** Symmetric to Case 2.

**Case 4.** Assume first that $R$ has an ancestor with a $\bullet$-pebble. Then by Lemma 3.6, we have

$$(\boldsymbol{r}_{U_0} - \boldsymbol{r}_{V_0}) - (\boldsymbol{r}_S - \boldsymbol{r}_X) - (\boldsymbol{r}_{S'} - \boldsymbol{r}_Y) - \sum_{i\in[k]} (\boldsymbol{r}_{U_i} - \boldsymbol{r}_{V_i}) = \mathbf{0}.$$

Since $\mathsf{L}(U_0) = \mathsf{L}(S) \sqcup \mathsf{L}(S') \sqcup \bigsqcup_{i\in[k]} \mathsf{L}(U_i)$, we obtain that

$$g_{U_0} - g_S - g_{S'} - \sum_{i\in[k]} g_{U_i} \geq (k+1)\cdot\Delta g \geq \Delta g > (\ell b + \ell u - u + 1)\cdot \max h > h_{V_0} + h_S + h_{S'} + \sum_{i\in[k]} h_{U_i},$$

where the last inequality holds since $S \neq U_i \neq U_j \neq S'$ for $i \neq j$, and the subtree $U_0$ has at most $\ell b + \ell u - u$ unary subtrees. Since $f, g, h$ take non-negative values and $\varphi_U - \varphi_V = g_U + h_U - h_V$ when $V$ is the unique child of $U$, we obtain that $\varphi$ satisfies the wall-crossing inequality

$$(\varphi_{U_0} - \varphi_{V_0}) - (\varphi_S - \varphi_X) - (\varphi_{S'} - \varphi_Y) - \sum_{i\in[k]} (\varphi_{U_i} - \varphi_{V_i}) > 0.$$

Assume now that $R$ has no ancestor with a $\bullet$-pebble. Then we have

$$(\boldsymbol{r}_S - \boldsymbol{r}_X) + (\boldsymbol{r}_{S'} - \boldsymbol{r}_Y) + \sum_{i\in[k]} (\boldsymbol{r}_{U_i} - \boldsymbol{r}_{V_i}) = \mathbf{0}.$$

The wall-crossing inequality is thus even easier to satisfy since $\varphi_{U_0} - \varphi_{V_0}$ does not appear.

**Case 5.** By Lemma 3.6, we have

$$\boldsymbol{r}_S + \boldsymbol{r}_{S'} - \boldsymbol{r}_R - \boldsymbol{r}_X = \mathbf{0}$$

Since $\mathsf{L}(R) = \mathsf{L}(S) = \mathsf{L}(S') = \mathsf{L}(X)$ and $\mathsf{B}(R) = \mathsf{B}(S) \sqcup \{\circ\} = \mathsf{B}(S') \sqcup \{\bullet\} = \mathsf{B}(X) \sqcup \{\circ, \bullet\}$, we have

$$\varphi_S + \varphi_{S'} - \varphi_R - \varphi_X = h_S + h_{S'} - h_R - h_R > 0. \qquad \blacksquare$$

***Remark 3.9*** Note that the conditions of Theorem 3.8 are just sufficient conditions to ensure the wall-crossing inequalities. To find functions satisfying these conditions, pick three arbitrary strictly submodular functions $f, g, h$ and

https://doi.org/10.4153/S0008414X25000094 Published online by Cambridge University Press

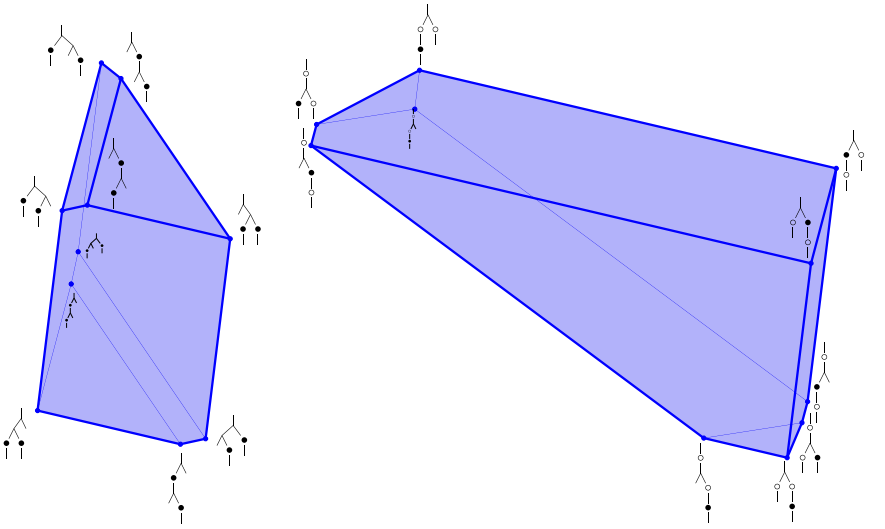


*Figure 14*: The pebble tree polytopes $\mathbb{PTP}_3^{0,1}$ (left) and $\mathbb{PTP}_2^{1,1}$ (right).

rescale first $g$ by a factor $4(\ell b + \ell u - u + 1) \cdot \max h / \Delta g$, and then $f$ by a factor $(\ell b + \ell u - u) \cdot (\max g + \max h)/\Delta f$. We just write $\mathbb{PTP}_\ell^{b,u}$ if we want to consider $\mathbb{PTP}_\ell^{b,u}(f, g, h)$ for arbitrary $f, g, h$ satisfying the conditions of Theorem 3.8.

***Example 3.10*** In the extreme situations of Example 2.1:

- the pebble tree fan $\mathcal{PF}_1^{b,u}$ (*a.k.a.* braid fan) is the normal fan of the classical permutahedron, which can be obtained for $h_B = \binom{b+1}{2} - \binom{|B|+1}{2}$ (the functions $f$ and $g$ are irrelevant here, since $[s, t]$ is constant to $[1]$),
- the pebble tree fan $\mathcal{PF}_\ell^{0,0}$ (*a.k.a.* sylvester fan) is the normal fan of the classical associahedron [SS93, Lod04], which can be obtained for $f_X = \binom{\ell+1}{2} - \binom{|X|+1}{2}$ (the functions $g$ and $h$ are irrelevant here, since $B$ is constant to $\varnothing$).

Figure 14 illustrates polytopal realizations of the pebble tree fans $\mathcal{PF}_3^{0,1}$ and $\mathcal{PF}_2^{1,1}$. Note that, while they have the same combinatorics by Proposition 2.10, their geometric realizations differ.

Finally, we translate the first three points of Proposition 2.10 and Remark 2.11 to pebble tree polytopes. Note that the last two transformations of Proposition 2.10 do not respect the geometry of the pebble tree polytopes.

***Proposition 3.11*** *Consider the operations of Definitions 2.2–2.4.*

(1) *The map defined by* $\boldsymbol{e}_{\ell j+i-\delta_{j\neq 0}} \mapsto \boldsymbol{e}_{\ell(j+1)-i}$ *for any* $(i, j) \in ([\ell] \times [0, b + u]) \backslash \{(\ell, 0)\}$ *induces an isometry of the pebble tree polytope* $\mathbb{PTP}_\ell^{b,u}(f, g, h)$.

(2) *If* $u > 1$, *the pebble tree polytope* $\mathbb{PTP}_\ell^{b,u}(f, g, h)$ *is a facet of the pebble tree polytope* $\mathbb{PTP}_\ell^{b+1,u-1}(f, g, h)$. *Hence,* $\mathbb{PTP}_\ell^{b,u}(f, g, h)$ *is a codimension* $u$ *face of* $\mathbb{PTP}_\ell^{b+u,0}(f, g, h)$.

https://doi.org/10.4153/S0008414X25000094 Published online by Cambridge University Press

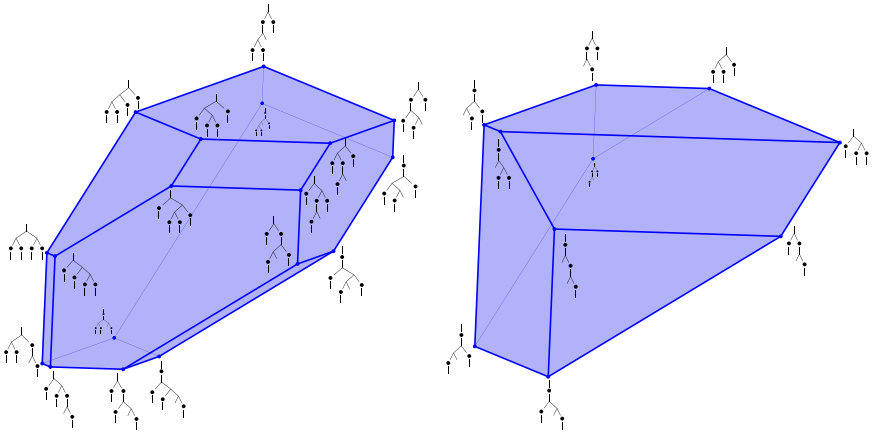


*Figure 15*: The $\alpha$-assocoipahedra for $\alpha = 01101$ (left) and $\alpha = 0001$ (right), realized as faces of the pebble tree polytopes $\mathbb{PTP}_4^{1,0}$ and $\mathbb{PTP}_3^{1,0}$.

(3) *The pebble tree polytope* $\mathbb{PTP}_\ell^{b,u}(f, g, h)$ *is a codimension* $\ell$ *face of the pebble tree polytope* $\mathbb{PTP}_\ell^{b+1,u}(f, g, h')$ *where* $h(X) = h'(\{x + 1 \mid x \in X\})$ *for* $X \subseteq [b + u]$.

***Remark 3.12*** Following Remarks 2.5, 2.11, and 2.18, observe that for any signature $\alpha \in \{1, 0\}^{\ell+1}$, the $\alpha$-assocoipahedron of [PT18] is realized by a face of the pebble tree polytope $\mathbb{PTP}_\ell^{1,0}$. For instance, Figure 15 shows faces of the pebble tree polytopes $\mathbb{PTP}_4^{1,0}$ and $\mathbb{PTP}_3^{1,0}$ which realize the $\alpha$-assocoipahedra for $\alpha = 01101$ and $\alpha = 0001$ presented in [PT18, Figures 8, 9, 14, and 15]. Note that the combinatorics of the 0001-assocoipahedra represented in Figure 15 (right) is also isomorphic to the pebble tree polytopes $\mathbb{PTP}_4^{0,1}$ represented in Figure 14 by combining Points (2) and (4) of Proposition 2.17.

## 4 Pebble tree numerology

In this section, we compute the generating functions of the maximal pebble trees (Section 4.1) and of all the pebble trees (Section 4.2), and gather explicit expansions of these generating functions (Section 4.3). While the methods are standard computations based on generatingfunctionology [FS09], the results reveal a few surprises. All references like A000108 are entries of the Online Encyclopedia of Integer Sequences [OEI10].

### 4.1 Enumeration of maximal pebble trees

We start with the enumeration of the maximal pebble trees which is significantly simpler.

***Definition 4.1*** For $\ell, u, b \in \mathbb{N}$, we denote by $m_\ell^{b,u}$ the number of maximal pebble trees of $\mathcal{P}_\ell^{b,u}$ (*i.e.,* with $\ell$ leaves, $b$ balanced and $u$ unbalanced colors). We consider

https://doi.org/10.4153/S0008414X25000094 Published online by Cambridge University Press

the generating function

$$\mathfrak{M}^{b,u}(x) := \sum_{\ell=1}^{\infty} m_\ell^{b,u}\, x^\ell.$$

***Proposition 4.1*** *The generating functions $\mathfrak{M}^{b,u}(x)$ satisfy the functional equations*

$$\mathfrak{M}^{b,u}(x) = x \cdot \delta_{b=0} + b \cdot \mathfrak{M}^{b-1,u+1}(x) + \sum_{\nu=0}^{u} \binom{u}{\nu} \cdot \mathfrak{M}^{b+\nu,u-\nu}(x) \cdot \mathfrak{M}^{b+u-\nu,\nu}(x),$$

*where $\delta$ is the Kronecker delta. Hence, $\mathfrak{M}^{b,u}(x)$ is algebraic for any $b, u \in \mathbb{N}$.*

**Proof** A maximal pebble tree in $\mathcal{P}^{B,U}_{[s,t]}$ is:

- either a leaf if $s = t$ and $B = \varnothing$,
- or a unary node with a single pebble colored by $\gamma \in B$ and a child in $\mathcal{P}^{B\setminus\{\gamma\},U\cup\{\gamma\}}_{[s,t]}$,
- or a binary node with no pebble and two children in $\mathcal{P}^{B,V}_{[s,r]}$ and $\mathcal{P}^{B,U\setminus V}_{[r,t]}$ for some $r \in [s,t]$ and $V \subseteq U$.

The functional equations for $\mathfrak{M}^{b,u}(x)$ are immediate consequences of this structural decomposition by classical generatingfunctionology [FS09]. The algebraicity of $\mathfrak{M}^{b,u}(x)$ follows as it belongs to a system of finitely many polynomial equations (all equations for a given sum $b + u$). ∎

***Example 4.2*** When $b = u = 0$, we recover the functional equation $\mathfrak{M}^{0,0}(x) = x + \mathfrak{M}^{0,0}(x)^2$ which yields the classical Catalan generating function

$$\begin{aligned}\mathfrak{M}^{0,0}(x) &= \frac{1-\sqrt{1-4x}}{2}\\ &= x + x^2 + 2x^3 + 5x^4 + 14x^5 + 42x^6 + 132x^7 + \cdots \quad (\texttt{A000108})\end{aligned}$$

***Example 4.3*** For $b + u = 1$, we obtain that

$$\mathfrak{M}^{1,0}(x) = \mathfrak{M}^{0,1}(x) + \mathfrak{M}^{1,0}(x)^2 \qquad \text{and} \qquad \mathfrak{M}^{0,1}(x) = x + 2 \cdot \mathfrak{M}^{1,0}(x) \cdot \mathfrak{M}^{0,1}(x)$$

from which we can compute the expansions

$$\mathfrak{M}^{1,0}(x) = x + 3x^2 + 16x^3 + 105x^4 + 768x^5 + 6006x^6 + 49152x^7 + \cdots \quad (\texttt{A085614})$$
$$\mathfrak{M}^{0,1}(x) = x + 2x^2 + 10x^3 + 64x^4 + 462x^5 + 3584x^6 + 29172x^7 + \cdots \quad (\texttt{A078531})$$

These functions actually both satisfy a cubic equation, namely

$$2 \cdot \mathfrak{M}^{1,0}(x)^3 - 3 \cdot \mathfrak{M}^{1,0}(x)^2 + \mathfrak{M}^{1,0}(x) - x = 0 \qquad \text{and}$$
$$4 \cdot \mathfrak{M}^{0,1}(x)^3 - \mathfrak{M}^{0,1}(x)^2 + x^2 = 0.$$

***Example 4.4*** For $b + u = 2$, we obtain

$$\mathfrak{M}^{2,0}(x) = 2 \cdot \mathfrak{M}^{1,1}(x) + \mathfrak{M}^{2,0}(x)^2, \tag{4.1}$$

$$\mathfrak{M}^{1,1}(x) = \mathfrak{M}^{0,2}(x) + 2 \cdot \mathfrak{M}^{2,0}(x) \cdot \mathfrak{M}^{1,1}(x), \tag{4.2}$$

$$\mathfrak{M}^{0,2}(x) = x + 2 \cdot \mathfrak{M}^{2,0}(x) \cdot \mathfrak{M}^{0,2}(x) + 2 \cdot \mathfrak{M}^{1,1}(x)^2. \tag{4.3}$$

https://doi.org/10.4153/S0008414X25000094 Published online by Cambridge University Press

From which we can compute the expansions:

$$\begin{aligned}
\mathfrak{M}^{2,0}(x) &= 2x + 24x^2 + 496x^3 + 12560x^4 + 354048x^5 + 10665088x^6 + \cdots \\
\mathfrak{M}^{1,1}(x) &= x + 10x^2 + 200x^3 + 5000x^4 + 140000x^5 + 4200000x^6 + \cdots \quad \texttt{(A156275)} \\
\mathfrak{M}^{0,2}(x) &= x + 6x^2 + 112x^3 + 2728x^4 + 75360x^5 + 2242304x^6 + \cdots
\end{aligned}$$

The expansion of $\mathfrak{M}^{1,1}(x)$ is quite surprising, but can be explained by a tiny functional miracle. Indeed, observe that we obtain that $2 \cdot \mathfrak{M}^{1,1}(x) = \mathfrak{M}^{2,0}(x) \cdot \big(1 - \mathfrak{M}^{2,0}(x)\big)$ from Equation (4.1) and that $\mathfrak{M}^{0,2}(x) = \mathfrak{M}^{1,1}(x) \cdot \big(1 - 2 \cdot \mathfrak{M}^{2,0}(x)\big)$ from Equation (4.2). Replacing $\mathfrak{M}^{0,2}(x)$ on both sides of Equation (4.3), we obtain

$$\begin{aligned}
\mathfrak{M}^{1,1}(x) &= x + 4 \cdot \mathfrak{M}^{1,1}(x) \cdot \mathfrak{M}^{2,0}(x) \cdot \big(1 - \mathfrak{M}^{2,0}(x)\big) + 2 \cdot \mathfrak{M}^{1,1}(x)^2 \\
&= x + 10 \cdot \mathfrak{M}^{1,1}(x)^2. \qquad (4.4)
\end{aligned}$$

This shows that $m_\ell^{1,1} = 10^{\ell-1} C_\ell$, where $C_\ell = \frac{1}{\ell+1}\binom{2\ell}{\ell}$ is the Catalan number.

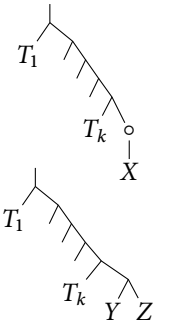
Consider the map sending a maximal pebble tree of $\mathcal{P}_\ell^{1,1}$ to its underlying binary tree. In view of the formula $m_\ell^{1,1} = 10^{\ell-1} C_\ell$, it is natural to expect that its fibers all have size $10^{\ell-1}$. However, while the size of the fiber of a binary tree $T$ is clearly invariant under reordering the children of $T$, it is not constant on all binary trees already for $\ell = 4$. Namely, the fiber of the binary tree whose children are both the tree on 2 leaves contains 968 pebble trees of $\mathcal{P}_4^{1,1}$, while the fiber of each of the remaining 4 binary trees on 4 leaves contains 1008 pebble trees of $\mathcal{P}_4^{1,1}$.

Despite this disappointing observation, one can provide a bijective explanation for the appearance of the Catalan numbers in $m_\ell^{1,1}$. It requires the following observation.

***Example 4.4*** Any maximal ∘-balanced •-unbalanced pebble tree can be uniquely obtained from a right comb by attaching

- to each left leaf, a maximal $\{\circ, \bullet\}$-balanced pebble tree,
- to the right leaf, a maximal ∘-balanced •-unbalanced pebble tree, whose root is
  - either a unary node with a ∘ pebble, whose unique child $X$ is $\{\circ, \bullet\}$-unbalanced,
  - or a binary node with no pebble, whose left child $Y$ is ∘-balanced •-unbalanced and whose right child $Z$ is $\{\circ, \bullet\}$-balanced.

These two options are illustrated on the right. A similar decomposition holds with a left comb instead of a right comb.




We now proceed to define, for $\ell, r \geq 1$, an explicit bijection $\psi$ sending a triple $(T, L, R)$ of maximal pebble trees of $\mathcal{P}_2^{1,1}$, $\mathcal{P}_\ell^{1,1}$, and $\mathcal{P}_r^{1,1}$ respectively to a maximal pebble tree of $\mathcal{P}_{\ell+r}^{1,1}$. The image $\psi(T, L, R)$ is described in Figure 16. Note that $\psi(T, L, R)$ sometimes depends on the type of $L$ or $R$ in the sense of the decomposition of Remark 4.5. In this description, we denote by $T_\bullet$ the •-balanced ∘-unbalanced pebble tree obtained by exchanging the ∘ and • pebbles in a ∘-balanced •-unbalanced pebble tree $T$. As the decomposition of Remark 4.5 is unique, the map $\psi$ is well defined,

https://doi.org/10.4153/S0008414X25000094 Published online by Cambridge University Press

and it is immediate to check that the resulting trees are maximal pebble trees of $\mathcal{P}^{1,1}_{\ell+r}$. Again by Remark 4.5, it is straightforward to check that $\psi$ is bijective. Finally, as $m^{1,1}_2 = 10$, the existence of the bijection $\psi$ directly implies Equation (4.4), hence the fact that $m^{1,1}_\ell = 10^{\ell-1}C_\ell$.

## 4.2 Enumeration of all pebble trees

We now consider all pebble trees.

***Definition 4.2*** For $\ell, n, u, b \in \mathbb{N}$, we denote by $p^{b,u}_{\ell,n}$ the number of pebble tree with $\ell$ leaves, $n$ nodes, $b$ balanced and $u$ unbalanced colors. We consider the generating function

$$\mathfrak{P}^{b,u}(x,y) := \sum_{\ell=1}^{\infty}\sum_{n=0}^{\infty} p^{b,u}_{\ell,n}\, x^\ell\, y^n.$$

***Proposition 4.6*** *The generating functions $\mathfrak{P}^{b,u}(x,y)$ satisfy the functional equations*

$$\mathfrak{P}^{b,u}(x,y) = x\cdot\delta_{b=0} + y\cdot\sum_{s=1}^{b}\binom{b}{s}\cdot\mathfrak{P}^{b-s,u+s}(x,y) + y\cdot\sum_{\substack{d\geq 2\\ X_1,\dots,X_b\\ Y_1,\dots,Y_u}}\prod_{k=1}^{d}\mathfrak{P}^{b_k,u_k}(x,y)$$

*where $\delta$ is the Kronecker delta, where each $X_i$ ranges among arbitrary subsets of $[d]$ while each $Y_j$ ranges among strict subsets of $[d]$, and where $b_k := |\{i\in[b] \mid k\in X_i\}| + |\{j\in[u] \mid k\in Y_j\}|$ and $u_k := b+u-b_k$ for any $k\in[d]$. Hence, $\mathfrak{P}^{b,u}(x)$ is algebraic for any $b,u\in\mathbb{N}$.*

**Proof** A pebble tree of $\mathcal{P}^{B,U}_{[s,t]}$ is:

- either a leaf if $s=t$ and $B=\varnothing$,
- or a unary node with some pebbles colored by a non-empty subset $S\subseteq B$ (one pebble of each color in $S$) and a child in $\mathcal{P}^{B\setminus S,U\cup S}_{[s,t]}$,
- or a node with some pebbles and $d\geq 2$ children in $\mathcal{P}^{B_1,U_1}_{[s_1,t_1]},\dots,\mathcal{P}^{B_d,U_d}_{[s_d,t_d]}$ respectively, for some $s=s_1\leq t_1=s_2\leq\cdots\leq t_d=t$ and $B_i\subseteq B$ and $U_i\subseteq U$ for all $i\in[d]$, such that $\bigcap_{i\in[d]}U_i=\varnothing$.

The functional equations for $\mathfrak{P}^{b,u}(x)$ are immediate consequences of this structural decomposition by classical generatingfunctionology [FS09]. The algebraicity of $\mathfrak{P}^{b,u}(x)$ follows as it belongs to a system of finitely many polynomial equations (all equations for a given sum $b+u$). ∎

***Example 4.7*** When $b=u=0$, we recover the functional equation

$$\mathfrak{P}^{0,0}(x,y) = x + \frac{y\cdot\mathfrak{P}^{0,0}(x,y)^2}{1-\mathfrak{P}^{0,0}(x,y)}$$

which yield the classical Schröder generating function

$$\begin{aligned}\mathfrak{P}^{0,0}(x,y) &= \frac{y\left(x+y-\sqrt{x^2-2xy-4xy^2+y^2}\right)}{2(1+y)}\\ &= x + x^2y + x^3(y+2y^2) + x^4(y+5y^2+5y^3) + x^5(y+9y^2+21y^3+14y^4) + \cdots\end{aligned}$$

https://doi.org/10.4153/S0008414X25000094 Published online by Cambridge University Press

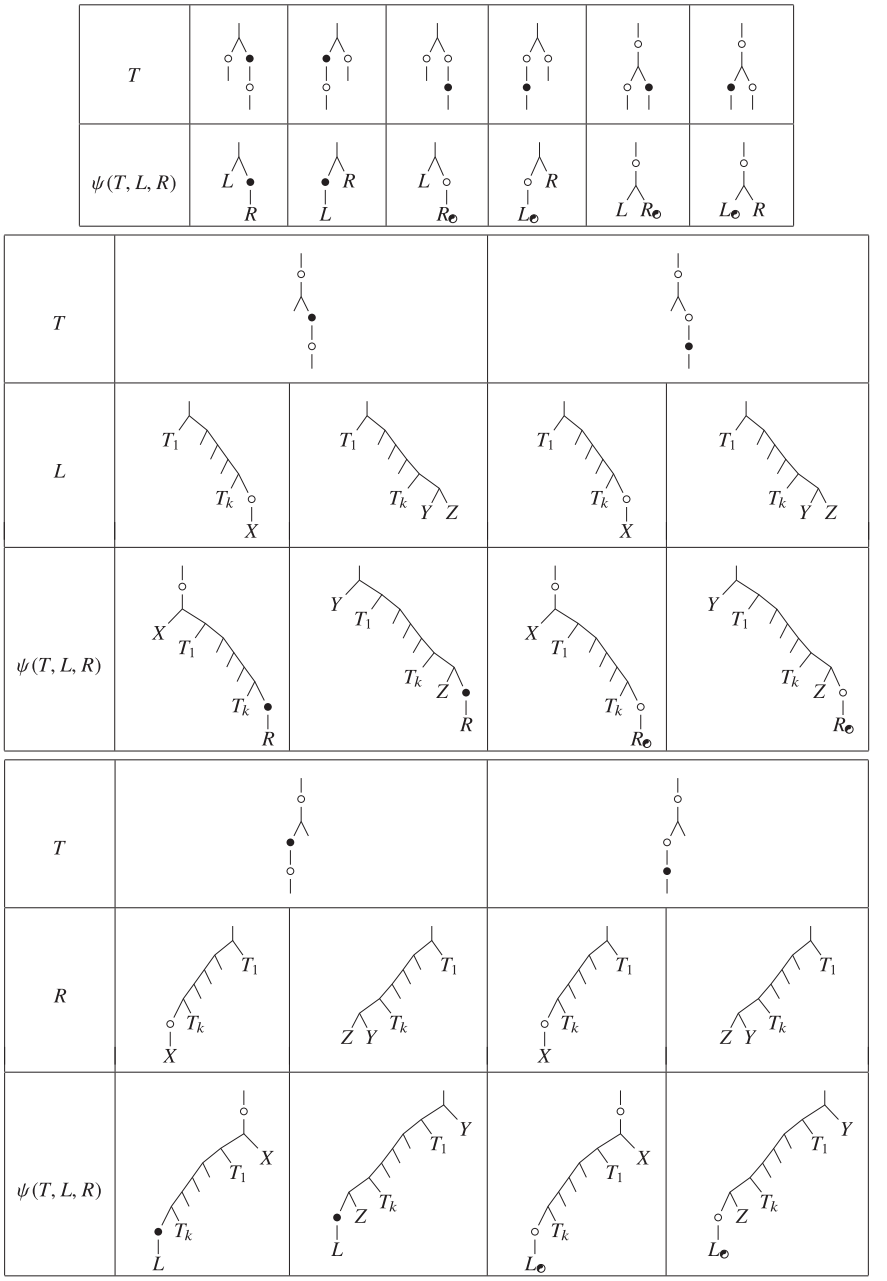



*Figure 16*: Bijection $\psi$ sending a triple $(T, L, R)$ of maximal pebble trees of $\mathcal{P}_2^{1,1}$, $\mathcal{P}_\ell^{1,1}$ and $\mathcal{P}_r^{1,1}$ respectively to a maximal pebble tree of $\mathcal{P}_{\ell+r}^{1,1}$.

https://doi.org/10.4153/S0008414X25000094 Published online by Cambridge University Press

The expansions of the generating functions $\mathfrak{P}^{b,u}(x,1)$ and $\mathfrak{P}^{b,u}(x,y)$ for $b+u\le 2$ can be found in Section 4.3. Finally, we observe that the evaluations of $\mathfrak{P}^{b,u}(x,y)$ at $y=1$ and $y=-1$ have a geometric meaning.

***Proposition 4.8*** *For any $b,u\in\mathbb{N}$, the evaluation $\mathfrak{P}^{b,u}(x,1)$ is the generating function of the total number of faces of the pebble tree polytope $\mathbb{PTP}_\ell^{b,u}$, and*

$$\mathfrak{P}^{b,u}(x,-1)=\frac{x}{(-1)^b+(-1)^u x}.$$

**Proof** By Theorem 3.8, $p_{\ell,n}^{b,u}$ is the number of $(\ell+\ell b+\ell u-u-2-n)$-dimensional faces of the $(\ell+\ell b+\ell u-u-2)$-dimensional pebble tree polytope $\mathbb{PTP}_\ell^{b,u}$. This implies that

- $\sum_n p_{\ell,n}^{b,u}$ is the total number of faces of $\mathbb{PTP}_\ell^{b,u}$,
- $\sum_n p_{\ell,n}^{b,u}(-1)^n=(-1)^{\ell+\ell b+\ell u-u-2}$ by Euler's formula.

This immediately implies the statement. ∎

## 4.3 Expansions of generating functions

Below are the expansions of the generating functions $\mathfrak{M}^{b,u}(x)$, $\mathfrak{P}^{b,u}(x,1)$ and $\mathfrak{P}^{b,u}(x,y)$ of Definitions 4.1 and 4.2 for all $b+u\le 2$.

$b=0$ and $u=0$.

$$\mathfrak{M}^{0,0}(x)=x+x^2+2x^3+5x^4+14x^5+42x^6+132x^7+\cdots \quad (\texttt{A000108})$$
$$\mathfrak{P}^{0,0}(x,1)=x+x^2+3x^3+11x^4+45x^5+197x^6+903x^7+\cdots \quad (\texttt{A001003})$$
$$\mathfrak{P}^{0,0}(x,y)=x+x^2y+x^3(y+2y^2)+x^4(y+5y^2+5y^3)+x^5(y+9y^2+21y^3+14y^4)+\cdots$$

$b=1$ and $u=0$.

$$\mathfrak{M}^{1,0}(x)=x+3x^2+16x^3+105x^4+768x^5+6006x^6+49152x^7+\cdots \quad (\texttt{A085614})$$
$$\mathfrak{P}^{1,0}(x,1)=x+7x^2+81x^3+1151x^4+18225x^5+308519x^6+5465313x^7+\cdots$$
$$\mathfrak{P}^{1,0}(x,y)=xy+x^2(y+3y^2+3y^3)+x^3(y+8y^2+24y^3+32y^4+16y^5)+\cdots$$

$b=0$ and $u=1$.

$$\mathfrak{M}^{0,1}(x)=x+2x^2+10x^3+64x^4+462x^5+3584x^6+29172x^7+\cdots \quad (\texttt{A078531})$$
$$\mathfrak{P}^{0,1}(x,1)=x+3x^2+33x^3+459x^4+7185x^5+120771x^6+2129169x^7+\cdots$$
$$\mathfrak{P}^{0,1}(x,y)=x+x^2(y+2y^2)+x^3(y+7y^2+15y^3+10y^4)+\cdots$$

$b=2$ and $u=0$.

$$\mathfrak{M}^{2,0}(x)=2x+24x^2+496x^3+12560x^4+354048x^5+10665088x^6+\cdots$$
$$\mathfrak{P}^{2,0}(x,1)=3x+115x^2+7431x^3+587591x^4+51702219x^5+4860786491x^6+\cdots$$
$$\mathfrak{P}^{2,0}(x,y)=x(y+2y^2)+x^2(y+9y^2+33y^3+48y^4+24y^5)+\cdots$$

https://doi.org/10.4153/S0008414X25000094 Published online by Cambridge University Press

$b = 1$ and $u = 1$.

$$\mathfrak{M}^{1,1}(x) = x + 10x^2 + 200x^3 + 5000x^4 + 140000x^5 + 4200000x^6 + \cdots \quad (\texttt{A156275})$$
$$\mathfrak{P}^{1,1}(x,1) = x + 33x^2 + 2061x^3 + 160797x^4 + 14049369x^5 + 1315182201x^6 + \cdots$$
$$\mathfrak{P}^{1,1}(x,y) = xy + x^2(y + 7y^2 + 15y^3 + 10y^4) + \cdots$$

$b = 0$ and $u = 2$.

$$\mathfrak{M}^{0,2}(x) = x + 6x^2 + 112x^3 + 2728x^4 + 75360x^5 + 2242304x^6 + 70084864x^7 + \cdots$$
$$\mathfrak{P}^{0,2}(x,1) = x + 13x^2 + 765x^3 + 58297x^4 + 5031129x^5 + 467426661x^6 + \cdots$$
$$\mathfrak{P}^{0,2}(x,y) = x + x^2(y + 6y^2 + 6y^3) + \cdots$$

**Acknowledgements** I am grateful to Doriann Albertin for discussions around Example 4.4 and for a very constructive proofreading, to Wenjie Fang for pointing out Remark 2.6 and for discussions on Propositions 4.1 and 4.6, to Guillaume Laplante-Anfossi for motivating me to find polytopal realizations of the assocoipahedra, to Thibaut Mazuir for algebraic discussions on the assocoipahedra, and to Anna de Mier, Jordi Castellví Foguet and Clément Requilé for discussions on Example 4.4 during the 3rd Workshop on Geometric, Algebraic and Probabilistic Combinatorics in Monserrat on July 2022. Finally, I am grateful to an anonymous referee for useful suggestions on the presentation of this paper. This research benefited from computations and tests done using the open-source mathematical software `Sage` [Sd16] and its combinatorics features developed by the `Sage-combinat` community [SCc16], and from the Online Encyclopedia of Integer Sequences [OEI10].

## References

[CFZ02] F. Chapoton, S. Fomin, and A. Zelevinsky, *Polytopal realizations of generalized associahedra*. Canad. Math. Bull. **45**(2002), no. 4, 537–566.
[CP22] F. Chapoton and V. Pilaud, *Shuffles of deformed permutahedra, multiplihedra, constrainahedra, and biassociahedra*. Annales Henri Lebesgue, **7**(2024), pp. 1535–1601.
[CS99] M. Chas and D. Sullivan, *String topology*. Preprint, 1999, arXiv:math/9911159.
[CS03] R. Cori and G. Schaeffer, *Description trees and Tutte formulas*. Theoret. Comput. Sci. **292**(2003), no. 1, 165–183. Selected papers in honor of Jean Berstel.
[DRS10] J. A. De Loera, J. Rambau, and F. Santos, *Triangulations: Structures for algorithms and applications*. volume 25 of Algorithms and Computation in Mathematics, Springer Verlag, Berlin, 2010.
[For08] S. Forcey, *Convex hull realizations of the multiplihedra*. Topol. Appl. **156**(2008), no. 2, 326–347.
[FS09] P. Flajolet and R. Sedgewick, *Analytic combinatorics*, Cambridge University Press, Cambridge, 2009.
[JS98] B. Jacquard and G. Schaeffer, *A bijective census of nonseparable planar maps*. J. Combin. Theory Ser. A **83**(1998), no. 1, 1–20.
[Lod04] J.-L. Loday, *Realization of the Stasheff polytope*. Arch. Math. (Basel) **83**(2004), no. 3, 267–278.
[OEI10] The on-line encyclopedia of integer sequences. Published electronically at http://oeis.org, 2010.
[Pos09] A. Postnikov, *Permutohedra, associahedra, and beyond*. Int. Math. Res. Not. **6**(2009), 1026–1106.
[Pou14] L. Pournin, *The diameter of associahedra*. Adv. Math. **259**(2014), 13–42.
[PP18] V. Pilaud and V. Pons, *Permutrees*. Algebr. Comb. **1**(2018), no. 2, 173–224.

https://doi.org/10.4153/S0008414X25000094 Published online by Cambridge University Press

[PRW08] A. Postnikov, V. Reiner, and L. K. Williams, *Faces of generalized permutohedra*. Doc. Math. **13**(2008), 207–273.
[PS19] V. Pilaud and F. Santos, *Quotientopes*. Bull. London Math. Soc. **51**(2019), no. 3, 406–420.
[PT18] K. Poirier and T. Tradler, *The combinatorics of directed planar trees*. J. Combin. Theory Ser. A **160**(2018), 31–61.
[SCc16] The Sage-Combinat community, *Sage-Combinat: enhancing Sage as a toolbox for computer exploration in algebraic combinatorics*. 2016. http://wiki.sagemath.org/combinat.
[Sd16] The Sage developers, *Sage mathematics software*, 2016. http://www.sagemath.org.
[SS93] S. Shnider and S. Sternberg, *Quantum groups: From coalgebras to Drinfeld algebras*. Series in Mathematical Physics, International Press, Cambridge, MA, 1993.
[Sta70] J. Stasheff, *H- spaces from a homotopy point of view*. Lecture Notes in Mathematics, 161, Springer-Verlag, Berlin, 1970.
[STT88] D. D. Sleator, R. E. Tarjan, and W. P. Thurston, *Rotation distance, triangulations, and hyperbolic geometry*. J. Amer. Math. Soc. **1**(1988), no. 3, 647–681.
[TZ07] T. Tradler and M. Zeinalian, *Algebraic string operations*. K- Theory **38**(2007), no. 1, 59–82.
[Zie98] G. M. Ziegler, *Lectures on polytopes*, volume 152 of Graduate texts in Mathematics, Springer-Verlag, New York, 1998.

*Departament de Matemàtiques i Informàtica, Universitat de Barcelona & Centre de Recerca Matemàtica, Barcelona, Spain*
*e-mail*: vincent.pilaud@ub.edu

https://doi.org/10.4153/S0008414X25000094 Published online by Cambridge University Press